Asynchronous Cooperative Optimization of a Capacitated Vehicle Routing Problem Solution

Luca Accorsia, Demetrio Laganab, Federico Michelottoc, Roberto Musmannob, Daniele Vigoc, d

^aGoogle, Erika-Mann-Straße 33, Munich, 80636, Bavaria, Germany
 ^bDIMEG, University of Calabria, Via Pietro Bucci, 87036 - Rende (CS), Italy
 ^cDEI "G. Marconi", University of Bologna, Viale del Risorgimento 2, 40136 - Bologna, Italy
 ^dCIRI-ICT, University of Bologna, via Quinto Bucci, 336, 47521 - Cesena, Italy

Abstract

We propose a parallel shared-memory schema to cooperatively optimize the solution of a Capacitated Vehicle Routing Problem instance with minimal synchronization effort and without the need for an explicit decomposition. To this end, we design $FILO2^x$ as a single-trajectory parallel adaptation of the FILO2 algorithm originally proposed for extremely large-scale instances and described in Accorsi and Vigo (2024). Using the locality of the FILO2 optimization applications, in $FILO2^x$ several possibly unrelated solution areas are concurrently asynchronously optimized. The overall search trajectory emerges as an iteration-based parallelism obtained by the simultaneous optimization of the same underlying solution performed by several solvers. Despite the high efficiency exhibited by the single-threaded FILO2 algorithm, the computational results show that, by better exploiting the available computing resources, $FILO2^x$ can greatly enhance the resolution time compared to the original approach, still maintaining a similar final solution quality for instances ranging from hundreds to hundreds of thousands customers.

Keywords: Capacitated Vehicle Routing Problem, Parallel Metaheuristics, Large-Scale Instances

1. Introduction

The Vehicle Routing Problem (VRP) (Dantzig and Ramser 1959, Toth and Vigo 2002, Semet et al. 2014) is an NP-hard combinatorial optimization problem that is widely studied in the field of operations research, both for its notorious difficulty and its wide range of applications in freight and people transportation. The VRP aims to find the least-cost routes that visit exactly once each customer in a given set. The VRP has different variants depending on the objectives and constraints. The most studied is the Capacitated Vehicle Routing Problem (CVRP) (Toth and Vigo 2002, Semet et al. 2014), in which routes are performed by a fleet of homogeneous vehicles with limited capacity. The CVRP is formally defined on an undirected graph G = (V, E), where V is the set of vertices and $E = \{(i, j) \in V \times V : i < j\}$ is the set of edges. The vertex set V is partitioned into $V = \{0\} \cup V'$, where vertex 0 represents the depot and $V' = \{1, \ldots, N\}$ is the vertex set associated with N customers. A nonnegative cost c_{ij} is associated with each edge $(i, j) \in E$. Moreover,

Email addresses: accorsi@google.com (Luca Accorsi), demetrio.lagana@unical.it (Demetrio Laganà), federico.michelotto2@unibo.it (Federico Michelotto), roberto.musmanno@unical.it (Roberto Musmanno), daniele.vigo@unibo.it (Daniele Vigo)

we assume that the cost matrix $\mathbf{C} = \{c_{ij}, (i,j) \in E\}$ satisfies the triangle inequality. For a subset $V' \subseteq V$, we identify with $\mathcal{N}_i^k(V')$ the ordered list of the k nearest neighbor vertices $j \in V'$ of vertex i with respect to the cost matrix \mathbf{C} . If k = |V'|, we omit the apex k, that is, $\mathcal{N}_i(V')$. Each customer $i \in V'$ requires an integer quantity $q_i > 0$ of goods from the depot, and $q_0 = 0$. An unlimited fleet of homogeneous vehicles, each with capacity Q, is located at the depot to serve the customers. A CVRP solution $S = \{r_1, \ldots, r_h, \ldots, r_{|S|}\}$ is composed of |S| Hamiltonian circuits, called routes $r_h = \{i_0, i_1, \ldots, i_p, i_{p+1}\}$, starting from the depot (i.e., $i_0 = 0$), visiting a subset of customers $i_1, \ldots, i_p \in V'$, and returning to the depot (i.e., $i_{p+1} = 0$). A solution S is feasible for the CVRP if all customers are visited exactly once and none of the vehicles exceed their capacity. The cost of a route is defined as the total cost of the edges connecting the visited customers: $c_{r^h} = \sum_{j=0}^p c_{i_j i_{j+1}}$, while the cost c_S of a solution S is given by the sum of the costs of the routes of S: $c_S = \sum_{u=1}^{|S|} c_{r^u}$. The objective of the CVRP is to find a feasible solution with a minimum total cost.

The exact methods for the CVRP are based on branch-and-bound, branch-and-cut, branch-and-price, and dynamic programming (Semet et al. 2014) and, in the worst-case, they all require exponential time with respect to the input size (number of customers) to obtain an optimal solution. The high time complexity of exact methods makes them unsuitable for solving large-scale CVRP instances. To address this challenge, heuristic algorithms are employed, offering satisfactory solutions in a reasonable amount of time. Many heuristic algorithms consume a considerable amount of CPU time in the improvement phase. This results in a considerable degradation in performance when solving very large-scale instances.

In this work, we focus on reducing the computing time required to solve very small- and large-scale CVRP instances by implementing a scalable parallel computing approach. In general, parallel computing is a methodology for solving a specific problem by distributing the computational workload among multiple concurrent processes (solvers) on a set of processors (Crainic and Toulouse 2010). The objective is to distribute the computational load among different processors to enhance performance when the size of the problem increases. The workload to be distributed may concern the algorithm, the search space, or the problem structure. In the context of algorithmic workload distribution, the implementation of functional parallelism is a key objective. This approach involves the distribution of computations that require the most CPU time across available processors that execute parallel tasks utilizing the same data, with each task being allocated to a specific processor. These processors collaborate with one another, if required, to ensure the efficient utilization of the resources. The distribution of workload in terms of search space is achieved through the utilization of data parallelism, which involves the decomposition of the problem domain into smaller portions, with each parallel processor undertaking the processing of a specific portion. Finally, the distribution of the workload determined by the problem structure entails the decomposition of the problem into a series of subproblems. The subsequent tasks are either concerned with addressing these subproblems or with integrating their solutions into the original problem. In general, it is possible to define fine- and coarsegrained parallelisms in accordance with the small and large size of the tasks resulting from the decomposition of the problem. In the existing literature, two main strategies for the partitioning of search space are identified: domain decomposition and multisearch. Domain decomposition is explicit, while multisearch is implicit. More precisely, the domain decomposition strategy is characterized by explicit partitioning of the search space, whereas the multisearch strategy involves implicit segmentation through independent thread explorations of the search space. In the context of the multisearch method, a prevalent issue pertains to the non-overlapping exploration of the search space, a challenge that can be mitigated by employing different

search strategies. From an algorithmic perspective, the most elementary form of parallelism arises from the concurrent execution of inner loop iterations with synchronization components. However, it should be noted that this approach can result in substantial delays associated with the communication overhead required by the synchronization. The success of parallel/distributed metaheuristic for the VRP is based on the Cooperative Search (CS) paradigm (Alba 2005, Crainic 2005, Crainic and Hail 2005, Talbi 2006, Crainic and Toulouse 2008, Crainic 2008, Crainic and Toulouse 2010). Cooperative search uses multiple solution methods and cooperation mechanisms to share information asynchronously and generate new data. Cooperative-search strategies have several key aspects: i) the solution methods engaged in cooperation (including the same method with different parameter settings or populations); ii) the information shared (e.g., the best solution and status updates); iii) the way of sharing information and global search control; and iv) how the exchanged information is used globally and how each process uses the received information. In the context of parallel algorithms based on CS strategies for the CVRP, meta-heuristics such as Tabu Search (TS), Genetic and Evolutionary Algorithms (GEAs), Memetic Algorithms (MAs), Ant Colony Algorithms (ACOs) and Simulated Annealing (SA) methods have been shown to be particularly effective. The rationale behind the employment of these metaheuristics as a single-processor local search algorithm is primarily due to their ability to efficiently explore the search space while escaping from local minima, and to represent the CVRP solution as a set of paths or routes, which allows for easy updating through information exchange between processors that can optimize subsets of routes. Nevertheless, these metaheuristics are inherently limited in their ability to scale as the size of the instances increases, especially when a CVRP solution comprises a very large number of routes and the number of processors is either quite limited or quite large in relation to the number of routes. In the latter cases, particular attention is required for the mechanism by which information is shared and the subset of routes is updated. This inherent limitation shows up in the parallel algorithms, resulting in suboptimal efficiency and consequent degradation in the quality of the solutions obtained when these algorithms are used to solve very large CVRP instances. The present work aims to partially address this gap.

Our work contributes to the literature on parallel algorithms for the CVRP on the following grounds:

- we propose a parallel algorithm based on a shared-memory CS strategy whose execution results in a single-trajectory parallel adaptation of the FILO2 algorithm (Accorsi and Vigo 2024) that is executed by several solvers to simultaneously optimize localized solution areas;
- the proposed approach results in the coordinated optimization of a shared solution, without the need of decomposition nor the imposition of rigid boundaries on the solvers. Synchronization among solvers is minimized by using data redundancy and a message-passing communication;
- the computational results demonstrate the effectiveness of the parallel algorithm, which achieves results comparable with those obtained by the sequential FILO2 algorithm, but in a fraction of time, on a wide range of instance sizes.

The paper is organized as follows. In Section 2, we position our work with respect to the literature, while Section 3 provides the background of the FILO2 and FILO algorithms. We describe our solution approach in Section 4. In Section 5, we present the computational performance of our solution approach. Section 6 presents a computational analysis of the algorithm components. Finally, Section 7 concludes our work.

2. Literature Review

Parallel algorithms for the Traveling Salesman Problem (TSP) and VRPhave been researched for almost three decades. As this work focuses primarily on the CVRP, this section provides an overview of the main contributions to parallel and distributed algorithms for VRP.

The algorithms that achieved the best performance in parallel/distributed computing for solving very largescale instances of the VRP are based on decomposition techniques, as outlined in Kindervater and Lenstra (1986), Gendron and Crainic (1994), Alba (2005), Talbi (2006), Crainic et al. (2006), Crainic and Toulouse (2010). Decomposition-based methods are based on three subsequent stages. The first one is the Decomposition stage, which splits the original problem into sub-problems. In the Integration stage, the results of these sub-problems are combined to create solutions to the original problem. Finally, in the last stage the evolution of the complete method is defined. It is clearly essential that these mechanisms are explicitly adapted to align with the specific heuristic strategies adopted in the solution of sub-problems. In 2005, Crainic et al. (2005) presented a classification system for parallel metaheuristic strategies. The authors introduced three dimensions for controlling the global process and managing data. The first dimension is Search Control Cardinality, which delineates whether a singular (1C; 1-control) or multiple (pC; p-control) processes oversee the global search. The second dimension is Search Control and Communication, which describes the data exchange between processes: namely, Rigid Synchronization (RS), Knowledge Synchronization (KS), Collegial (C), and Knowledge Collegial (KC). The third dimension is the Search Differentiation, which concerns how searches are initialized and which search method is used. Four cases have been identified in this respect: SPSS (Same Initial Point/Population, Same Search Strategy), SPDS (Same Initial Point/Population, Different Search Strategy), MPSS (Multiple Initial Point/Population, Same Search Strategy), and MPDS (Multiple Initial Point/Population, Different Search Strategy). Within this nomenclature, the following parallel search strategies can be defined. Low-Level 1-Control Parallelization Strategies are used by exact or heuristic methods. These strategies are based on a rigid synchronization between the master process and other processes, and are implemented in the traditional master-slave parallel programming model, where communication between slave processes is prohibited with the objective of accelerating the search process. The Neighborhood-based, 1-Control/Rigid Synchronization/Same Initial Point, Same Search Strategy approach enables the parallelization of the neighborhood search between processes. A neighborhood solution can be generated and evaluated independently, facilitating parallelization. This can be achieved through the classical master-slave mechanism. The Independent Multi-Search (IMS) is a p-Control parallelization strategy that involves multiple searches on the entire search space, starting from the same or different initial solutions, with the objective of selecting the best solution at the end. The IMS is a pC/RS class with multiple starting points/populations that implements a MPSS search strategy. The Cooperative Search strategies (Crainic and Toulouse 2010) advance IMS methods by allowing data sharing throughout the search. The data exchange mechanism helps achieve better results than standalone multisearch techniques. The data-sharing cooperation mechanism specifies how different search threads interact.

Search processes may exchange data directly or indirectly, typically through a blackboard repository. Blackboard repositories store information from all processes and can be used as a source of information accessible to all processes. Cooperation can be classified as synchronous or asynchronous. In synchronous cooperation, referred to as p-Control Knowledge Synchronization (pC/KS) strategy, processes share knowledge about solutions at a pre-determined time. The p-Control Collegial (pC/C) strategy is a fully distributed one, with

cooperation actions initiated independently by search processes. When the pC/C communication strategy is used to modify the knowledge of specific processes, it results in a p-Control Knowledge Collegial (pC/KC). In accordance with the classification system outlined above, the following analysis examines the most recent contributions to the scientific literature concerning CVRP.

Doerner et al. (2004) explores the application of Ant Colony Optimization (ACO) for solving the CVRP and evaluates three ACO paradigms: Rank-Based Ant System (ASrank), Max-Min Ant System (MMAS), and Ant Colony System (ACS). The approach can be classified as a pC/RS strategy due to the structured communication between processors and synchronized pheromone updates. The computational analysis is based on 14 standard VRP benchmark instances taken from Christofides et al. (1979). These instances comprise between 50 and 199 customers, with the configurations including both random customer locations on a plane and locations included in clusters. A comparison is conducted between the three ACO paradigms (ASRank, MMAS and ACS) by measuring the relative percentage deviation from the best known solutions. An analysis of several algorithm settings is conducted in terms of the average and worst results over five runs from the best known solutions. The average deviation of ASRank, MMAS, and ACS is 0.97, 0.80, and 1.22, respectively, when using the best setting. In order to analyze the effectiveness of the parallel algorithm, the speedup and efficiency are measured for varying numbers of processors. The speedup is defined as $S_p = \frac{T_{seq}}{T_p}$, where S_p is the speedup obtained on p processors, T_{seq} is the measured sequential execution time and T_p is the parallel execution time on p processors. The implementation of this speedup measure, using eight processors, has been demonstrated to result in a sixfold enhancement in efficiency for problem instances involving 150 customers.

Kalatzantonakis et al. (2005) investigates the impact of cooperation strategies in parallel General Variable Neighborhood Search (GVNS) algorithms for solving the CVRP. Three parallelization models are proposed:

- non-cooperative model (NCM): pC/RS/SPSS, featuring rigid synchronization with no solution exchange among parallel processes;
- managed cooperative model (MCM): pC/C/SPSS, enabling asynchronous solution sharing through a centralized manager, promoting intensification;
- parameterized cooperative model (PCM): pC/KC/SPSS, with asynchronous and selective solution sharing that adapts dynamically based on search progression, optimizing both intensification and diversification.

All computational tests are carried out on 76 instances of the CVRPLIB library available at http://vrp.atd-lab.inf.puc-rio.br, with the number of customers varying from 32 to 360. In order to ensure a fair comparison and evaluation of the performance and quality of the solutions, all experiments are repeated ten times, and the average gap values of each parallel model are reported compared to the best-known solution values. Specifically, NCM presents an average gap of 0.837%, MCM of 1.260%, and PCM of 0.729%, thus demonstrating that PCM is the best approach, producing high-quality solutions. All parallel algorithms successfully achieve the optimum value for 14 out of 65 instances. No analysis in terms of speedup is presented, and none of the existing datasets, including larger instances, is examined in the computational testing.

Barbucha (2011) investigates the solution of CVRP using a genetic algorithm based on a team of hetero-

geneous cooperating agents within a multi-agent system framework. The proposed approach employs an asynchronous team paradigm, where agents represent various local search heuristics and collaborate to iteratively refine a shared population of solutions stored in global memory. The methodology corresponds to a pC/KC strategy because of its asynchronous cooperation and the reliance on shared memory for solution refinement. Computational experiments are carried out on 5 test instances of the Christofides et al. (1979) containing 50–199 customers and only the capacity constraint. The quality of the solutions is measured in terms of relative deviation from the best-known solution. The team of heterogeneous cooperative agents achieved an average deviation of 0.87%, compared to the best-known solution on all instances. No information on speedups is provided in the paper.

Barbucha (2014) presents a hybrid approach to solve the CVRP by integrating cooperative multiple neighborhood search with a multi-agent system (MAS) paradigm. This approach can be classified as a pC/KC strategy due to its distributed processes, asynchronous communication, and reliance on shared memory for solution exchange. The experiments are carried out on CVRP instances derived from Christofides et al. (1979), with a number of customers ranging from 50 to 199. The population size is set at 30 individuals and the algorithm terminates after 180 seconds of execution elapsed without improvement. The quality of the solutions is measured as Mean Relative Error (MRE) when compared to the optimal or best known solution, as reported by Laporte et al. (2000). The MRE (in %) from the best known solution is reported, calculated separately for cases where a single agent or a team of optimizing agents is involved in the search process and ranges between 2.27% and 3.57%. The work does not present any analysis in terms of speedup performance.

A parallel micro genetic algorithm for solving the CVRP is proposed in Borčinová (2018). The approach employs a coarse-grained parallelization strategy where each node executes a micro genetic algorithm on a small population, and synchronization occurs through a master node that collects the best solutions from all nodes and broadcasts the best global solution. The methodology is a pC/RS strategy due to its structured master-slave communication model, where nodes synchronize at defined intervals to exchange and update the global best solution. The experiments make use of 16 problems drawn from the sets (A and P) of benchmark problems by Augerat et al. (1995). The instances vary in size, with number of customers (including the depot) ranging from 16 to 101. The quality of the solutions is assessed by computing the relative deviation of the solution value from the known optimal costs. The average relative deviation from the optimal solution values, when employing the random generation of the initial solution, is 0.14, and is reduced to 0.07 when utilizing the parameterized Clarke-Wright algorithm. However, no information is provided regarding the potential speedups achieved with the parallel implementation.

In Abdelatti and Sodhi (2020) an innovative GPU-accelerated genetic algorithm for solving the CVRP is illustrated. By leveraging NVIDIA's CUDA architecture, the algorithm achieves high-speed parallel computations. It incorporates 2-opt local search and advanced population management techniques to enhance solution quality and prevent premature convergence. The methodology aligns with a pC/KC classification. The performance of the algorithm is evaluated using 14 common CVRP benchmarks, selected from various sources (Augerat et al. 1995, Christofides et al. 1969, 1981, Fisher 1994, Gillett and Johnson 1976, Li et al. 2005). These benchmarks range in size from 16 to 76 vertices. To assess the performance of the GPU-based algorithm, the authors used a CPU-only based implementation of their algorithm. Each algorithm is executed ten times on each benchmark problem, and averaged results are reported. The quality of the solutions

obtained is evaluated by computing the percentage of the gap, defined as $\left(\frac{s_0-s^*}{s^*}\right) \times 100$, where s_0 is the best solution obtained by the algorithm in 10 runs and s^* is the best known solution from the literature. The speedups of the GPU version over the CPU range from 52.7 times for the 21-node problem to 454.4 times for the 76-node problem. The gap obtained on instances with a number of customers between 60 and 76 ranges from 7.86% to 10.23%. The evaluation of the proposed algorithm for larger problems is lacking.

Yelmewad and Talawar (2021) propose a GPU-based parallelization of Local Search Heuristic (LHS) algorithms to efficiently solve the CVRP for large-scale instances. The parallelization is implemented at two levels: route-level and customer-level designs. The route-level approach assigns each route to a GPU thread, while the customer-level approach assigns a thread to each customer, significantly increasing computational parallelism. The approach can be classified as a pC/KC strategy. This classification reflects the asynchronous nature of the parallelization, where GPU threads independently explore solution neighborhoods and periodically update global memory to share improved solutions. The experimental analysis is carried out on the following CVRP data sets: the M set of Christofides et al. (1979) instances, Golden et al. (1998) instances, Li et al. (2005) instances, Kytöjoki et al. (2007) instances, Uchoa et al. (2017) instances, and the Arnold et al. (2019) instance set. The instance sizes thus range from 101 to 30,000 customers, exhibiting a wide spectrum of complexity and magnitude. On the Uchoa et al. (2017) data set, the route-level parallel strategy achieves a speedup that is 1.11 times faster in the worst-case, 4.40 times faster in the best-case and 2.17x on average compared to the sequential version for the same data set. No information on gap values compared with the best known solutions is provided. When compared with the sequential version on the Uchoa et al. (2017) data set, the customer-level parallel strategy is 1.99 times faster in the worst-case, 9.83 times on average, and 22.97 times in the best-case. Considering the sequential version on the Arnold et al. (2019) instances, the customer-level parallel strategy obtains speedups of 29.9, 83.52, and 147.20 times in the worst, average, and best-case, respectively. Finally, the speedup achieved in the worst, average, and best-case is 1.99, 4.69, and 9.03 times, respectively, compared with the route level parallel design. No gap value with respect to the best known solutions is reported since the LHS used in parallel strategies is not able to produce competitive results compared with the state of the art method.

Rajesh Pandian et al. (2023) introduces ParMDS, an efficient shared-memory parallel method for solving the CVRP. ParMDS employs a novel combination of Minimum Spanning Tree and Depth-First Search heuristics with randomization to generate candidate solutions quickly. The method is classified as a pC/KC strategy because of its asynchronous parallelization and solution sharing through memory. The ParMDS is tested on 130 instances of the CVRP from the CVRPLIB library, with sizes ranging from 76 to 30,000 customers and vehicle capacities between 3 and 2210. These instances include different sets, including the $\mathbb X$ and $\mathbb B$ datasets proposed by Uchoa et al. (2017) and Arnold et al. (2019). The quality of the solution is measured by the % gap. The ParMDS achieves a geometric mean deviation of 11.85% from the best known solutions related to two largest input instances per type, thereby significantly improving on the two baselines that implement a metaheuristic algorithm for VRP on GPU in CUDA, and a genetic algorithm for VRP on GPU, respectively. ParMDS, which is based on shared parallelization via OpenMP, demonstrates a significant speedup compared to baseline GPU implementations, varying between $36 \times$ and $1189 \times$. However, the comparison with the BKSs is limited to very few large instances, and the quality of solutions compared to the BKSs turns out to be rather poor.

3. Background: The FILO2 and FILO Algorithms

The parallel solution approach we propose, named $FILO2^x$, builds upon the FILO2 algorithm introduced by Accorsi and Vigo (2024), an efficient randomized metaheuristic designed to solve extremely large-scale CVRP instances in relatively short computing times. To facilitate the description of $FILO2^x$, this section first provides an overview of the main components of the FILO2 algorithm. Interested readers are referred to the original paper for further details.

FILO2 is an evolution of the FILO algorithm originally proposed in Accorsi and Vigo (2021) for the efficient resolution of large-scale CVRP instances with several thousand customers. FILO2 shares the same structure as FILO but replaces some computationally expensive procedures and memory-demanding data structures to make the resolution of extremely large-scale instances with up to one million customers approachable with ordinary computer systems.

The main strength of the FILO and FILO2 approaches consists in the iterative optimization of localized solution portions through the application of a sophisticated local search engine making use of heuristic acceleration and pruning techniques. Several local search operators such as the CROSS exchange (see Taillard et al. (1997)), the 2-opt (see Reinelt and Rinaldi (1994)), and the ejection chain (see Glover (1996)) are applied in a variable neighborhood descent fashion (VND, see Mladenović and Hansen (1997)). Their neighborhoods are efficiently explored using the static move descriptors (SMD) framework, originally proposed by Zachariadis and Kiranoudis (2010) and Beek et al. (2018), which cleverly exploits the locality of local search changes to avoid the re-evaluation of unrelated local search moves. In addition, neighborhoods are granular (see Toth and Vigo (2003)) and their size is dynamically adjusted with a vertex-wise sparsification factors to better control local search strength and intensify it to specific areas that require it the most. Finally, the optimization is localized to a limited set of vertices stored in a selective vertex cache to concentrate the search on recently modified solution areas. By combining these techniques, FILO2 and FILO exhibit a computing time that grows linearly with instance size and state-of-the-art results on well-studied literature datasets.

Algorithm 1 outlines the high-level structure of the FILO and FILO2 approaches. First, the construction

Algorithm 1 High-level structure of FILO and FILO2

```
1: procedure FILO(\mathcal{I}, s)

2: \mathcal{R} \leftarrow RANDOMENGINE(s)

3: S \leftarrow CONSTRUCTION()

4: k \leftarrow GREEDYROUTESESTIMATE(\mathcal{I})

5: if |S| > k then S \leftarrow ROUTEMIN(S, \mathcal{R})

6: S \leftarrow COREOPT(S, \mathcal{R})

7: return S

8: end procedure
```

Input parameters: instance \mathcal{I} , seed s

phase builds an initial feasible solution using a variation of the savings algorithm proposed by Clarke and Wright (1964). Then, the improvement phase refines this solution through the optional application of a route minimization procedure, followed by the core optimization procedure. The following paragraphs will provide more details on these two key phases of the FILO algorithms.

3.1. Instance Preprocessing

Before optimization can start, some data structures must be initialized. In particular, the instance under examination is preprocessed and the cost matrix C and the neighbor lists $\mathcal{N}_i(V)$, $i \in V$ are defined. These data structures will be extensively used during all the algorithm procedures.

3.2. Construction Phase

The initial feasible solution is built using an adaptation of the savings algorithm proposed by Arnold et al. (2019) to solve large-scale instances. In particular, rather than computing the savings score for all pairs of customers, which would require memory and computing time growing quadratically with the number of customers, only a limited number of pairs are considered. More precisely, for each customer i, savings are computed only for pairs (i, j) where j is among the $n_{cw} = 100$ nearest customers to i.

3.3. Improvement Phase

The initial solution generated by the construction phase is then possibly improved during the improvement phase. First, a route minimization procedure is potentially applied if the number of routes of the initial solution is greater than a heuristic estimate obtained by a greedy first-fit solution of the bin-packing problem associated with the CVRP instance. Then, the core optimization procedure, which represents the core part of the algorithm, is applied to the resulting solution for a predefined number of iterations.

Both the route minimization and the core optimization procedures are based on the iterated local search paradigm (see Lourenço et al. (2003)) and work by reoptimizing, through the local search engine mentioned in Section 3, a localized area disrupted by ruin-and-recreate applications. The route minimization procedure may evaluate partial solutions to more effectively compact routes. In contrast, the core optimization procedure exclusively explores the feasible space, employing a simulated annealing acceptance rule (see Kirkpatrick et al. (1983)) to achieve an effective diversification.

3.3.1. The Route Minimization Procedure

The route minimization procedure tries to compact the initial solution, but still favors quality over a lower number of routes. Algorithm 2 shows the pseudo-code of the procedure.

First, the current reference solution S is set to be equal to the current best-found solution S^* generated by the construction phase (line 2). The main loop is then executed for at most Δ_{RM} iterations and consists of (a) removing from S the customers belonging to a selected pair of routes (r_i, r_j) (lines 4 and 5), (b) sorting any unserved customers either randomly or based on their increasing demand, (c) potentially greedily inserting any removed customer in the position of S that minimizes the solution cost increase (lines 8 to 19), and finally, (d) applying local search to S (line 21).

The main peculiarity of this procedure consists, during step (c), of probabilistically leaving unserved customers that cannot be inserted into the existing routes because this would violate their load (lines 13 to 17). When this happens, such customers can be left unserved for the current iteration with a probability drawn from a uniform real distribution U(0,1) that decreases exponentially over the iterations (line 26). These customers will be considered in the subsequent iteration in steps (b) and (c).

The solution obtained after the local search application in step (d) will then replace S^* if it serves all customers and has a better cost or has the same cost but a lower number of routes (line 22). Indeed, the

Algorithm 2 Route minimization procedure

```
1: procedure ROUTEMIN(\mathcal{I}, S^*, k, \mathcal{R})
          S \leftarrow S^*, \mathcal{P} \leftarrow 1, L \leftarrow []
 2:
 3:
          for n \leftarrow 1 to \Delta_{RM} do
               (r_i, r_j) \leftarrow \text{PickPairOfRoutes}(S, \mathcal{R})
 4:
 5:
               S \leftarrow S \setminus r_i \setminus r_j
 6:
               L \leftarrow [L, \text{CustomersOf}(r_i, r_j)]
               \bar{L} = []
 7:
 8:
               for i \in \text{Ordered}(L, \mathcal{I}, \mathcal{R}) do
                    p \leftarrow \text{BestInsertionPositionInExistingRoutes}(i, S)
 9:
10:
                     if p \neq none then
                         S \leftarrow \text{Insert}(i, p, S)
11:
12:
                     else
13:
                         if |S| < k \vee U(0,1) > \mathcal{P} then
                              S \leftarrow \text{BuildSingleCustomerRoute}(i, S)
14:
15:
                               \bar{L} \leftarrow [\bar{L}, i]
16:
17:
                         end if
                     end if
18:
19:
               end for
                L \leftarrow \bar{L}
20:
21:
                S \leftarrow \text{LocalSearch}(S, \mathcal{R})
               if |L| = 0 \land (Cost(S) < Cost(S^*) \lor (Cost(S) = Cost(S^*) \land |S| < |S^*|)) then
22:
23:
                     S^* \leftarrow S
                    if |S^*| \leq k then return S^*
24:
25:
                end if
26:
               \mathcal{P} \leftarrow \text{Decrease}(\mathcal{P})
               if Cost(S) > Cost(S^*) then S \leftarrow S^*
27:
28:
           end for
          return S^*
29:
30: end procedure
```

Input parameters: instance \mathcal{I} , solution S^* , route estimate k, random engine \mathcal{R} , uniform real distribution U(0,1)

main goal of the procedure, which follows the CVRP objective function, is still to find good quality solutions rather than only reducing the number of routes. However, on average, the route minimization procedure proved to be effective in both quickly improving and compacting initial solutions.

3.3.2. The Core Optimization Procedure

The core optimization procedure is the main tool for improving the quality of the solution. Algorithm 3 shows the pseudocode of the procedure.

Initially, the current reference solution S is set equal to the current best-found solution S^* , generated by the construction phase, possibly followed by the route minimization procedure (line 2). Then, the main loop is performed for Δ_{CO} iterations. At each iteration, a neighbor solution S' is generated by applying a shaking and a local search procedure to the current reference solution S (lines 6 to 8). The generated neighbor S' will replace the best-found solution S^* whenever the former has a better quality (line 10). In addition, S' may replace the current reference solution S according to a standard simulated annealing criterion (line 16).

The ruin-and-recreate-based shaking procedure first removes a number of ω_i customers identified by a random walk on the graph underlying the solution, starting from a randomly selected seed customer i. The removed customers are then sorted by increasing or decreasing distance from the depot, decreasing demand value, or randomly shuffled, and sequentially reinserted in the position that minimizes their insertion cost. The parameters $\boldsymbol{\omega} = (\omega_1, \dots, \omega_{|V_c|})$ define the ruin intensity per customer. They are initially set at a value

Algorithm 3 Core optimization procedure

```
1: procedure CoreOpt(S^*, \mathcal{R})
            S \leftarrow S^*, \mathcal{T} \leftarrow \mathcal{T}_0
 2:
 3:
            \boldsymbol{\omega} \leftarrow (\omega_1, \omega_2, \dots, \omega_{|V_c|}), \omega_i \leftarrow \omega_{base} \ \forall i \in V_c
 4:
            \gamma \leftarrow (\gamma_0, \gamma_1, \dots, \gamma_{|V_c|}), \gamma_i \leftarrow \gamma_{base} \ \forall i \in V
            for n \leftarrow 1 to \Delta_{CO} do
 5:
                  S' \leftarrow S
 6:
                  S' \leftarrow \operatorname{Shaking}(S', \mathcal{R}, \boldsymbol{\omega})
 7:
                  S' \leftarrow \text{LocalSearch}(S', \mathcal{R})
 8:
                  if Cost(S') < Cost(S^*) then
 9:
                        S^* \leftarrow S'
10:
                       RESETSPARSIFICATIONFACTORS(\gamma)
11:
                  else
12:
                        UpdateSparsificationFactors(\gamma)
13:
14:
                  UPDATESHAKINGPARAMETERS(\omega, S', S, \mathcal{R})
15:
                  if Cost(S') < Cost(S) - \mathcal{T}log(U(0,1)) then S \leftarrow S'
16:
17:
18:
            end for
19:
            return S
20: end procedure
```

Input parameters: solution S^* , random engine \mathcal{R} , uniform real distribution U(0,1)

 $\omega_{base} = \lceil \ln |V| \rceil$ and iteratively updated for the customers involved in the ruin step, based on the quality of the resulting neighbor solution S' with respect to the initial source solution S. In particular, ω_i for customer i involved in the ruin step are increased if S and S' have a similar cost, they are decreased if S' has a much higher cost than S, and finally they are randomly changed otherwise. This allows for an iterative fine-tuning of the ruin intensity based on the search trajectory and on the instance and solution structure.

Another set of parameters $\gamma = (\gamma_0, \dots, \gamma_{|V_c|})$ defines the local search intensification level. The value $\gamma_i \in [0,1], i \in V$ determines a vertex-specific sparsification level ruling the number of move generators used during a local search application involving the vertex i. In particular, granular neighborhoods are defined by the set of move generators $T = \bigcup_{i \in V} \{(i,j), (j,i) \in E : j \in \mathcal{N}_i^{n_{gs}}(V \setminus \{i\})\}$, which identifies the arcs that connect i to its n_{gs} neighbors j, for every vertex i. The parameters γ_i allow the selection of a fraction of the least cost move generators for every vertex i.

The core optimization procedure begins with $\gamma_i = \gamma_{base}$, $i \in V$ (line 4), with γ_{base} being the base sparsification factor such that at least $n_{gs} \cdot \gamma_{base}$ move generators are always considered for every vertex. Whenever the best known solution S^* is replaced by a better neighbor solution S', the parameters γ_i for the vertices i involved in the last local search application are reset to γ_{base} (line 11). If, on the other hand, a vertex i is involved in a certain number of consecutive unsuccessful local search applications, the value of γ_i is set to $\gamma_i = min\{\gamma_i \cdot \lambda, 1\}$, where λ is an increment factor (line 13).

3.4. Design Highlights

In the following, we highlight some FILO and FILO2 design choices that are key ingredients of the proposed parallel approach.

3.4.1. Localized Optimization Pattern

The key principle of the FILO approaches is the localization of the optimization performed during the iterations of the improvement procedures. This is achieved by employing a technique called selective vertex caching, which allows the local search step to mainly re-optimize the area disrupted by the ruin-and-recreate

application. To this end, a cache tracks the vertices involved in the disruption process. At the beginning of every improvement procedure iteration, the cache is empty, as no action has been performed yet. The shaking application causes some vertices involved in the ruin-and-recreate procedure to be inserted into the cache. Subsequent local search applications are then only started from move generators having at least one of the endpoints in such a cache. Moreover, whenever a change is successfully applied to a solution (for example, due to the execution of an improving move during the exploration of a neighborhood), related vertices are inserted into the cache.

The cache has a limited size of C vertices, and it is managed with a least-recently changed eviction policy to constantly keep the optimization focused on more recently changed areas. This technique, which is also the basis for the design of the proposed parallel algorithm $FILO2^x$, is the main factor that localizes the iterations of the improvement procedures and therefore makes them extremely efficient and largely independent of the actual size of the instance.

3.4.2. Incremental Solution Synchronization

One of the critical changes introduced in FILO2 to manage extremely large-scale instances is related to the management of solution copies. In particular, due to the localized optimization pattern described in Section 3.4.1, the difference between a reference solution S and a neighboring solution S' is usually negligible as the size of the instance increases. Thus, in purely practical terms, performing a full linear-time solution copy (see, for example, lines 6 and 16 of Algorithm 3) may be incredibly expensive and largely unnecessary. For this reason, FILO2 replaces the copy operation with an incremental synchronization between solutions.

The construction phase generates the best-found solution S^* . An identical reference solution S is then obtained by performing the only complete copy executed by the entire algorithm. Any subsequent change to the current reference solution S is stored in the so-called do- and undo-lists. Possible changes to a solution can in practice be reduced to the following actions: insertion and removal of vertices, creation of one-customer routes, and deletion of empty routes.

The undo-list is used to restore a previous state of the reference solution by undoing part of the stored actions. This is particularly helpful in avoiding the explicit creation of an additional neighbor solution S'. In fact, the ruin, recreate and local search steps can be applied to the reference solution S, and later undone if the resulting neighbor is not accepted according to the chosen acceptance criteria. Similarly, the do-list is used to update the best-found solution S^* by applying all the actions that separate it from the current reference solution.

Synchronization between solutions is clearly no longer a linear-time procedure, but it is rather tied to the specific optimization pattern of the algorithm.

3.4.3. Reduced Memory Footprint

Another important difference introduced in FILO2 to scale to extremely large-scale instances consists in limiting the memory occupation of its data structures. More specifically, the cost matrix C is never explicitly stored, but the costs are computed on demand or retrieved from other existing data structures. For example, solutions keep track of the cost of their edges and, similarly, move generators provide the cost associated with their underlying edges to local search operators. Additionally, neighbor lists are limited to n_{nn} vertices that are identified by using a kd-tree built on top of vertex coordinates; see Bentley (1990).

4. The FILO2 x Solution Approach

In this section we describe $FILO2^x$, our proposed parallel solution approach for a timely resolution of small-to extremely large-scale CVRP instances. As will be better detailed in the following, the additional x superscript in the name denotes the usage of x FILO2-like algorithms, or simply solvers, to seamlessly optimize a common reference solution.

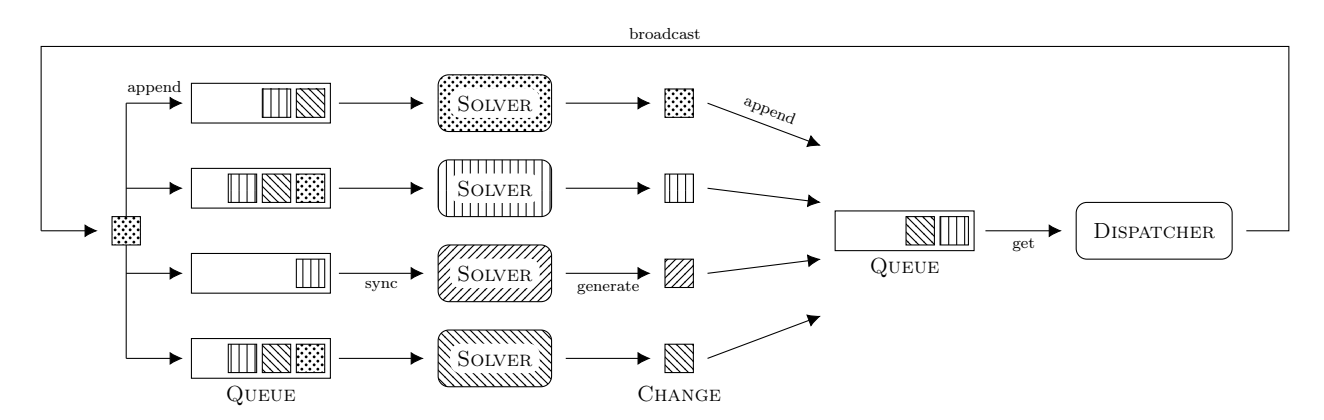
The main methodological contribution of our research consists in defining an efficient schema to allow an effective collaboration among the individual solvers aimed at collectively optimize a shared solution.

4.1. The Parallel Schema

 $FILO2^x$ represents the family of parallel solution approaches using x FILO2-based solvers to cooperatively and asynchronously optimize the same underlying solution. Ultimately, $FILO2^x$ results in the coordinated optimization of a shared solution, without the imposition of any guidance or rigid boundaries on the solvers. In particular, this is achieved by using data redundancy and message-passing communication for coordination while minimizing the need for inefficient synchronization.

Figure 1 shows a high-level representation of the proposed parallel schema. Initially, the desired number of

Figure 1: High-level $FILO2^x$ schema. Different filling patterns are used to associated candidate changes to the respective generator solver. Queues highlight how solvers may have not all applied the same amount of received changes, but changes in all queues are received in the same order.



solvers is created and initialized with the solution obtained through the construction phase and the greedy estimate of the required number of routes k; see Sections 3.2 and 3.3. Both the construction phase and the route estimation procedure do not require any solver-specific data structures, and as a design choice, they are performed before solvers are created. A different but equivalent choice could have been to execute them independently by all solvers.

As soon as they are created, the solvers asynchronously start to optimize their solution by running first the route minimization procedure described in Section 3.3.1 if required, followed by a parallel version of the core optimization procedure.

The route minimization procedure does require solver-specific data structures for the local search execution and it is thus performed by every solver independently. All solvers will however traverse the same search trajectory and converge to the same final solution as they are using a common seed for their pseudo-random number generator.

At every iteration of the parallel core optimization procedure, a candidate change is generated from the application of the ruin, recreate, and local search steps to the current reference solution. Candidate changes are sent to a centralized dispatcher component, which keeps them sorted according to their arrival time. The dispatcher actively and continuously retrieves the next available candidate change and broadcasts it to all available solvers. Candidate changes are evaluated by the solvers and possibly implemented to update their reference solution.

4.2. Memory Model

The FILO2 x algorithm employs a multithreaded shared memory architecture in which the solvers and the dispatcher are backed by a logical computer thread having its own independent execution flow.

Candidate changes generated by the solvers are stored into a shared thread-safe dispatcher queue data structure keeping them ordered according to a first-in first-out policy. The queue includes both improving and non-improving candidate changes. The latter are relevant for the simulated annealing acceptance criteria used in the core optimization phase (see line 16 of Algorithm 3).

The insertion of a new change into the queue is performed by the generating solver by first gaining exclusive access to the data structure through standard mutex locking mechanisms. Similarly, the removal of the least recent candidate change is performed by the dispatcher once access to the queue has been locked for the solvers. The dispatcher continuously retrieves the next available candidate change from the queue and broadcasts it to all solvers. When the queue is empty, the dispatcher suspends its execution, waiting for more changes.

Similarly, every solver manages a queue that stores in chronological order the candidate changes sent by the dispatcher. As for the dispatcher queue, exclusive access to the solver queue is required when the dispatcher adds a new change or when the solver retrieves the least recently available one.

4.3. Parallel Core Optimization Procedure

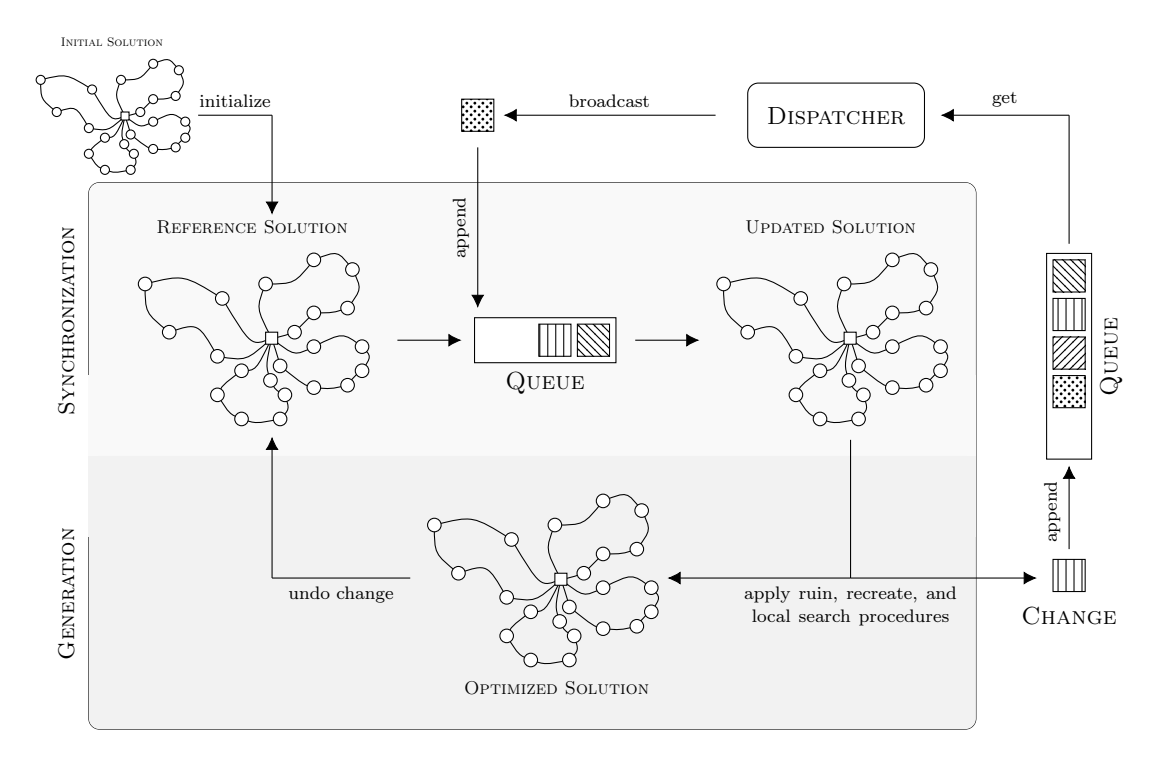
Every solver behaves as the single-threaded FILO2 algorithm described in Section 3. However, in addition, during the core optimization procedure, it leverages the work performed by other solvers to simulate the execution of the iterations they have already completed.

As depicted in Figure 2, once initialized with the solution obtained through the construction phase and possibly the route minimization procedure, a solver performs the parallel core optimization procedure through a sequence of synchronization and generation stages.

During the synchronization stage, some candidate changes in the solver queue are applied to its reference solution S to generate an updated reference solution S'. Note that, due to the concurrent and asynchronous nature of the algorithm, candidate changes keep flowing constantly to every solver queue. The update is thus limited to the sequence of changes available when the synchronization stage begins and does not include any additional received ones.

Each candidate change describes the effects of an iteration of the core optimization procedure on a reference solution through a list of actions; see Section 3.4.2. More precisely, a change contains the list of actions

Figure 2: Component activities during the parallel core optimization procedure. The solver is depicted by the gray box with the top lighter part representing the synchronization stage and the bottom darker one illustrating the generation stage.



associated with the ruin, recreate, and local search steps performed by some solver. Because a change may have been generated by a different solver on an arbitrarily different reference solution, the application of the associated actions to the current solver reference solution may produce an infeasible neighbor solution. For example, it may either generate a solution with route load constraints violations or even create customer sub-tours. Thus, before being applied, a candidate change is checked to verify whether it produces a feasible solution, and it is discarded otherwise.

Whenever a candidate change generates a feasible solution when applied to the current solver reference solution, an entire procedure iteration of Algorithm 3 (lines 5 to 18) is simulated with the ruin, recreate, and local search steps defined by the actions belonging to the change. The simulation includes the update of the algorithm parameters (lines 11, 13, and 15) and the possible update of the best-found and reference solutions (lines 10 and 16).

The generation stage consists of applying the ruin, recreate, and local search procedures to the updated reference solution S', resulting from the synchronization stage, to generate an optimized reference solution S''. The sequence of actions required to convert S' into S'' is recorded using the technique described in Section 3.4.2 and used to define a candidate change that is sent to the dispatcher.

Finally, the optimized solution S'' is reverted to S' by applying in reverse order the inverse actions that compose the generated candidate change (see Section 3.4.2), essentially bringing the current solver reference solution back to the same search trajectory traversed by all other solvers. The solver then returns to the synchronization stage with S = S' as the next reference solution.

The pseudo-random number generator of each solver is initialized with a different seed. Therefore, since

the ruin, recreate, and local search steps contain some randomization, each solver may produce different candidate changes during the generation stage. However, during the synchronization stage, a randomized update of the ω parameters may occur (see line 15 of Algorithm 3). To ensure that all solvers update these parameters consistently, a different pseudo-random number generator is instead initialized with the same seed for all the solvers.

4.4. Synchronization Mechanism

The dispatcher is the key component that guarantees the synchronization among solvers. Indeed, by collecting and relaying all candidate changes, it ensures all solvers receive them in the same absolute order, thus implicitly fixing a shared and unique search trajectory. Because solvers process received changes in the same order, they will always make the same decisions during the synchronization stage, eventually converging to the same final solution.

However, solvers may differ in the number of changes processed at a given time because of when they are scheduled by the operating system and due to their unique generation stage. At a specific time, they may thus be at different points on the same search trajectory, therefore causing their reference solutions to be possibly considerably different. This may induce the generation of candidate changes that, when applied by other solvers, might not produce feasible solutions. However, intuitively, as the size of the instance grows, given the localized optimization pattern used by the algorithm, the likelihood of defining these inapplicable changes decreases greatly, since different solvers will probably optimize different, and possibly disjoint, areas of the solution.

4.5. Parallel Instance Preprocessing

The initial instance preprocessing mentioned in Sections 3.1 and 3.4.3, which mainly consists of identifying n_{nn} neighbors for every vertex $i \in V$, can be very time consuming for extremely large-scale instances. In FILO2^x, once the kd-tree is built on top of the instance coordinates, the neighbors of the vertices are retrieved in parallel by employing x different threads. To make comparisons easier, we decided to link the number of threads employed during this preprocessing to the number of solvers used during the optimization. However, in principle, a different and greater number could profitably be employed.

5. Computational Results

The computational testing has the main objective of validating the strengths and limits of the proposed parallel approach. In particular, we assess whether FILO2 x is capable of finding solutions having a quality comparable to those obtained by FILO2, but in a fraction of time. To this end, we test the proposed algorithm on the well-known \mathbb{X} instances proposed by Uchoa et al. (2017), which are the current standard reference instances for the CVRP. In addition, we evaluate FILO2 x on the very large-scale \mathbb{B} instances presented by Arnold et al. (2019) and on the extremely large-scale \mathbb{I} instances introduced in Accorsi and Vigo (2024). Afterwards, in Section 6, we provide more insight into the behavior of the algorithm.

5.1. Implementation and Experimental Environment

The proposed FILO2^x algorithm was implemented in C++ and compiled using g++ 11.4. The experiments were executed on a 64-bit GNU/Linux Ubuntu 22.04 workstation with an Intel Xeon Gold 6254 CPU,

Table 1: Inherited main FILO2 parameters.

Scalability	
$n_{nn} = 1500$	Maximum number of nearest neighbors that are computed, stored and used during the algorithm execution.
C = 50	Maximum capacity of the selective vertex cache.
Initial solution definit	ion (construction phase and route minimization procedure)
$n_{cw} = 100$	Number of neighbors considered in the savings computation.
$\Delta_{RM} = 10^3$	Maximum number of route minimization iterations.
Granular neighborhoo	d
$n_{gs} = 25$	Number of neighbors considered for the definition of granular neighborhoods.
$\gamma_{base} = 0.25$	Base sparsification factor, i.e., at least $n_{gs}\cdot\gamma_{base}$ move generators are always considered for every vertex.
$\delta = 0.5$	Reduction factor used in the definition of the fraction of non-improving iterations performed before increasing a sparsification parameter.
$\lambda = 2$	Sparsification increment factor.
Core optimization pro	cedure
$\Delta_{CO} = 10^5, 10^6$	Number of core optimization iterations for short and long runs, respectively.
$\mathcal{T}_0,\mathcal{T}_f$	Initial and final simulated annealing temperatures.
$\omega_{base} = \lceil \ln V \rceil$	Initial shaking intensity.

running at 3.1 GHz, and equipped with 384 GB of RAM. The source code for $FILO2^x$ is available at https://github.com/acco93/filo2x.

For the experiments, we considered a standard version of FILO2 x and a longer version, called FILO2 x (long), performing 10^5 and 10^6 core optimization iterations, respectively. Given that FILO2 x is a randomized algorithm, to get a sense of the variability between executions, we performed a symbolic number of ten runs for each problem instance. All results and analyses described in the following sections refer to the average behavior of the algorithm.

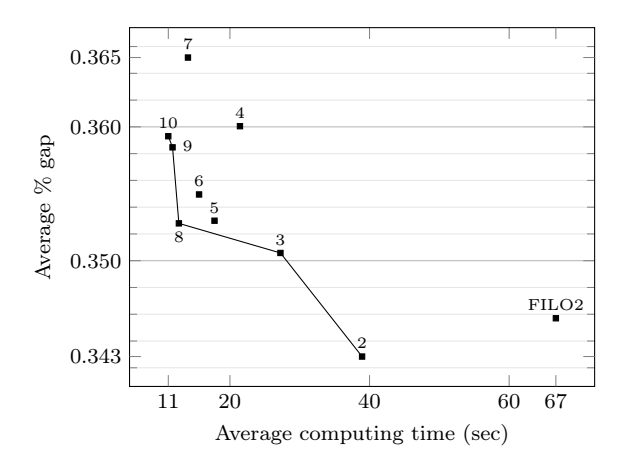
 $FILO2^x$ was compared to the original sequential algorithm FILO2, available at https://github.com/acco93/filo2. The results of FILO2 presented in this study were obtained by running the algorithm on the same machine described above. In addition, for reference, we include the results of state-of-the-art algorithms on the different studied datasets.

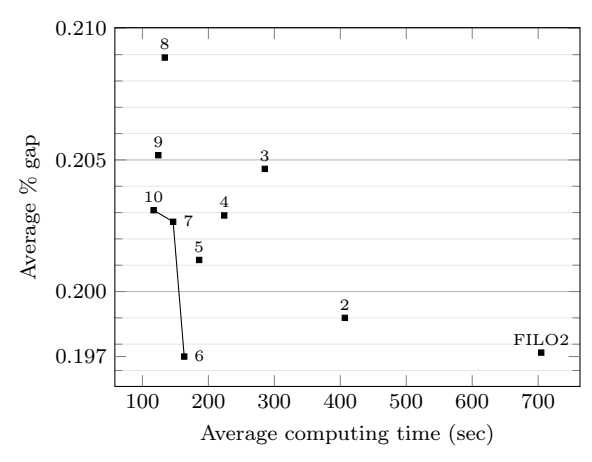
The best known solution values (BKS) for the \mathbb{X} and \mathbb{B} instances were taken from CVRPLIB (2025) at the time of writing, whereas the BKS for the \mathbb{I} instances come from Accorsi and Vigo (2024). The gaps are computed as $100 \cdot (z - \text{BKS})/\text{BKS}$ where z is the final solution value obtained by the algorithms, and the computing time is always reported in seconds. Finally, to ensure conciseness, in the following we opted to report only aggregated results. More details are included in the Appendix.

5.2. Parameter Tuning

To minimize behavioral differences between sequential and parallel versions, FILO2^x inherits all parameters and their values from the FILO2 sequential algorithm. Table 1 summarizes the inherited parameters, their value, and their meaning. In addition, FILO2^x uses a single supplementary parameter x defining the number of solvers used during optimization. Whenever x = 1, FILO2^x behaves similarly to FILO2. When x > 1, FILO2^x results in an emerging behavior that can be assimilated into a FILO2 approach in which multiple iterations of the core optimization procedure are executed in parallel. We tested values for x ranging from

Figure 3: Performance charts of FILO2^x and FILO2 on the \mathbb{X} dataset when performing standard (left) and long (right) runs. The individual numbers identify how many solvers have been used to run the FILO2^x algorithm.





2 to 10, as these values were found to provide the best performance on the specific machine and problem instances used in this study.

5.3. Testing on the X Instances

The X dataset, proposed by Uchoa et al. (2017), contains hundred instances with a number of customers ranging from 100 to 1000 modeling a wide range of customer demands and layout distributions. The X instances are the current reference benchmark literature dataset for the CVRP. Optimal or near-optimal solutions are known for most of the instances, and the best performing algorithms on this dataset usually differ in the order of a few percentage gap decimal points.

Although these small to large instances might not be the ideal candidates for parallel optimization, Figure 3 shows that the proposed parallel approach obtains competitive results in terms of final solution quality and an almost linear speedup when using up to five solvers. For experiments using more than five solvers, the computing time converges to approximately 10 seconds for short runs and 100 seconds for longer ones, indicating that for these instances and hardware configuration, more solvers cannot provide substantial speedup benefits.

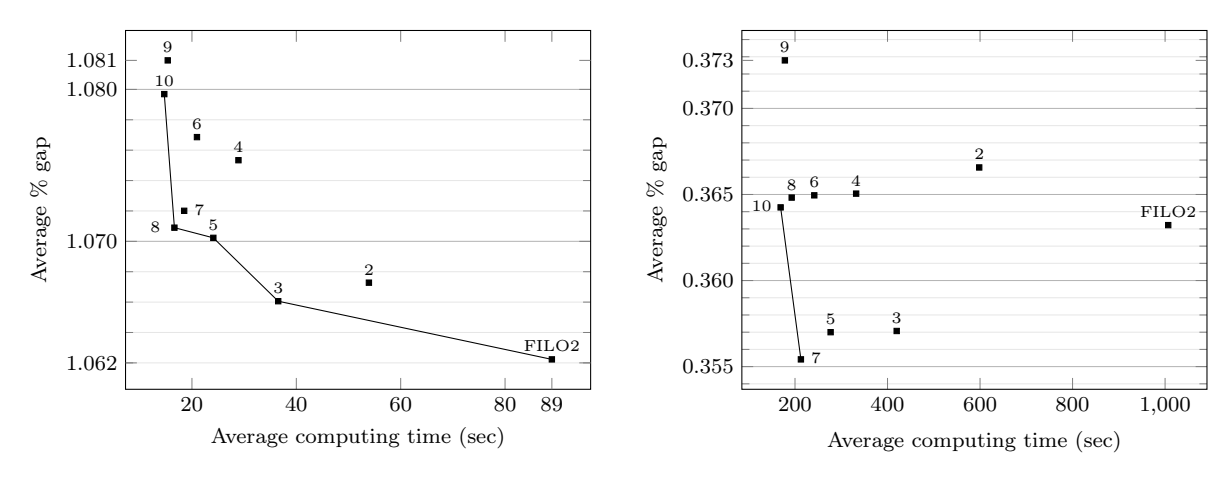
The graphs show small differences in the average percentage gap obtained by varying the number of solvers. However, statistical analyses of these results, detailed in Appendix A.1, show that the final solution quality obtained by the parallel versions is similar to that obtained by the original sequential algorithm.

Finally, to better frame the results obtained by FILO2 x , consider the hybrid genetic search (HGS) and the slack induction by string removals (SISR) algorithms proposed by Vidal (2022) and Christiaens and Vanden Berghe (2020), respectively, which are two of the most effective sequential algorithms for the CVRP. HGS and SISR obtain an average gap of 0.11% and 0.20%, respectively, when executed for $|V_c| \times 240/100$ seconds on the authors machines; see Vidal (2022).

5.4. Testing on the \mathbb{B} Instances

The \mathbb{B} dataset, introduced in Arnold et al. (2019), contains ten very large-scale instances with up to thirty thousand customers. These instances are modeled after real-world parcel distribution problems occurring in

Figure 4: Performance charts of FILO2^x and FILO2 on the $\mathbb B$ dataset when performing standard (left) and long (right) runs. The individual numbers identify how many solvers have been used to run the FILO2^x algorithm.



Belgium. In some instances, the depot is located centrally with respect to the customers and relatively short routes are needed to serve them. In other instances, the depot is eccentric with respect to the service zones, requiring much longer routes to visit the customers.

The performance charts shown in Figure 4 highlight that when performing standard runs, the sequential FILO2 algorithm provides solutions that have, on average, a slightly better quality compared to those obtained by the parallel version. On the other hand, when longer runs are performed, some parallel versions are able to provide better results. However, despite these minor differences, statistical analyses show that $FILO2^x$ and FILO2 both provide results of similar quality; see Appendix A.2.

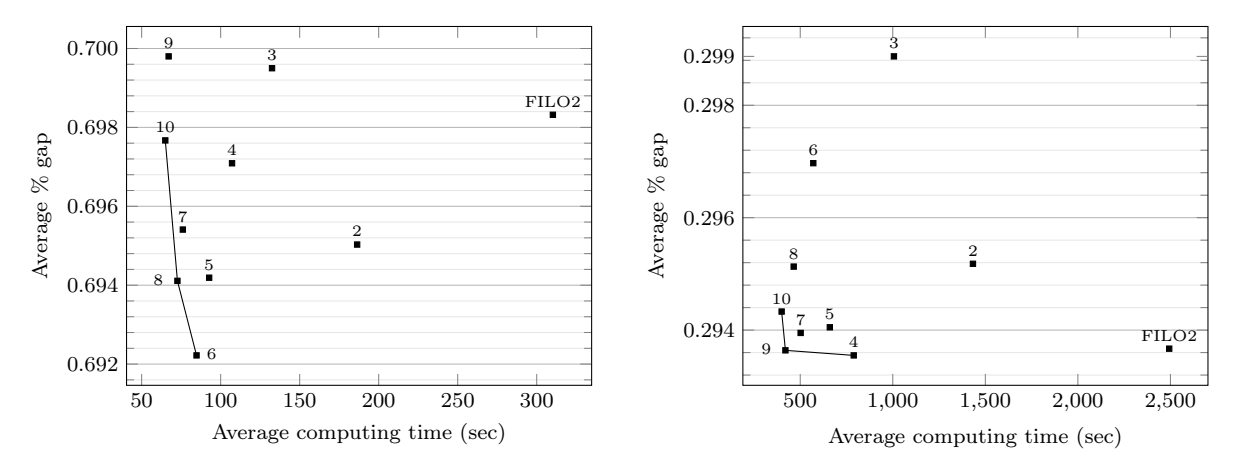
Finally, for a better comparison with state-of-the-art algorithms on this dataset, consider also the knowledge-guided local search algorithm for large-scale instances (KGLS^{XXL}) described in Arnold et al. (2019), which is a deterministic algorithm originally proposed to solve the $\mathbb B$ instances. Short runs of $|V_c|/1000\times180$ seconds of KGLS^{XXL} generate solutions having an average gap of 2.63%. Four times longer runs are capable of reducing the average gap to 1.77%. The percentage gaps are taken from Accorsi and Vigo (2024). Finally, Máximo et al. (2024) report an average gap of 0.10% obtained by their adaptive iterated local search heuristic, called AILS-II, in 600 minutes of computations.

5.5. Testing on the \mathbb{I} Instances

The I dataset, originally introduced in Accorsi and Vigo (2024), contains twenty extremely large-scale instances with a number of customers ranging from 20,000 to 1,000,000. These instances are based on projected coordinates of randomly sampled addresses in the various Italian regions with the depot located at the regional capital city position. The customer demand and the vehicle capacity are defined to have half of the instances where we can expect relatively short routes and half where longer ones are required.

Figure 5 compares the computational results of FILO2 x and FILO2. In contrast to what is happening for the other datasets, several parallel versions are capable of finding slightly better solutions during standard runs. The results for long runs align with those obtained on other datasets. However, as before, deeper statistical analyses show that the quality of the final solutions obtained by the parallel version does not differ from what the sequential algorithm can achieve; see Appendix A.3.

Figure 5: Performance charts of FILO2^x and FILO2 on the I dataset when performing standard (left) and long (right) runs. The individual numbers identify how many solvers have been used to run the FILO2^x algorithm.



6. Algorithmic Components Analysis

In this section, we provide more detailed analyses and interpretations of the algorithm behavior, strengths, and weaknesses. The analyses always consider computational results obtained by averaging ten distinct runs.

6.1. Speedup

The speedup, defined as the ratio between the computing times of the sequential and parallel versions, is a key property that justifies the design of a parallel approach. As described in Section 3, a sequential execution of FILO2 consists of (i) a preprocessing instance that sets up fundamental data structures, (ii) a construction phase that builds an initial feasible solution, (iii) a greedy estimation of the routes required by a solution, (iv) a possible application of the route minimization procedure and, finally, (v) the application of the core optimization procedure.

Steps (i) and (v) are the two most time consuming steps performed by the algorithm, with (i) being negligible when solving moderate size instances, but becoming extremely costly when approaching extremely large-scale ones. In particular, for standard FILO2 runs, (i) and (v) alone take more than 99% of the total computing time when solving the \mathbb{X} and \mathbb{B} instances. This value decreases to 94% when tackling the larger \mathbb{I} dataset. Clearly, when performing longer FILO2 runs, with ten times more core optimization procedure iterations, the time for (v) increases approximately tenfold, and (i) and (v) now take more than 99% of the total computing time for all datasets. Detailed statistics are available in the appendix in Tables A.5 and A.6 for the \mathbb{X} instances, A.14 and A.15 for the \mathbb{B} instances, and A.19 and A.20 for the \mathbb{I} instances.

FILO2^x takes advantage of multiple processors to parallelize these most time-consuming (i) and (v) procedures. Table 2 shows the speedup for these procedures averaged over instances and run configurations. For the \mathbb{B} and \mathbb{I} instances, we see an almost linear speedup of the instance preprocessing procedure. This is much less pronounced for the \mathbb{X} dataset, as this procedure already takes an incredibly short computing time of approximately 30 milliseconds when performed sequentially, and the time at this scale very often includes noise components not related to the algorithm (e.g., operating system routine operations). On the

Table 2: Speedup of the main algorithm procedures averaged over instances and run configurations for the different datasets. For reference, the Fraction column reports the percentage of time spent during the procedure, averaged across solvers. For the $\mathbb X$ instances we do not report results with 15 solvers as some of the smallest instances cannot be efficiently solved due to the high contention among solvers; see Section 6.2.

	Solvers	2	3	4	5	6	7	8	9	10	15	Fraction
\mathbb{X}	Instance preprocessing Core optimization	1.51 1.73	1.95 2.46	2.36 3.14	2.73 3.78	3.10 4.30	3.44 4.79	3.81 5.25	4.02 5.66	4.32 6.00	-	0.03 ± 0.00 99.07 ± 0.32
\mathbb{B}	Instance preprocessing Core optimization	1.87 1.68	$2.76 \\ 2.40$	3.64 3.03	$4.49 \\ 3.64$	$5.24 \\ 4.17$	$6.08 \\ 4.74$	$6.83 \\ 5.23$	$7.61 \\ 5.67$	$8.22 \\ 5.97$	$11.92 \\ 7.34$	$1.21 {\pm} 0.13$ $96.90 {\pm} 0.64$
I	Instance preprocessing Core optimization	1.91 1.74	2.88 2.48	3.78 3.18	4.70 3.81	5.52 4.42	6.50 5.04	7.28 5.47	8.27 6.06	9.00 6.38	13.49 8.27	$15.22 \pm 3.13 \\ 70.41 \pm 2.37$

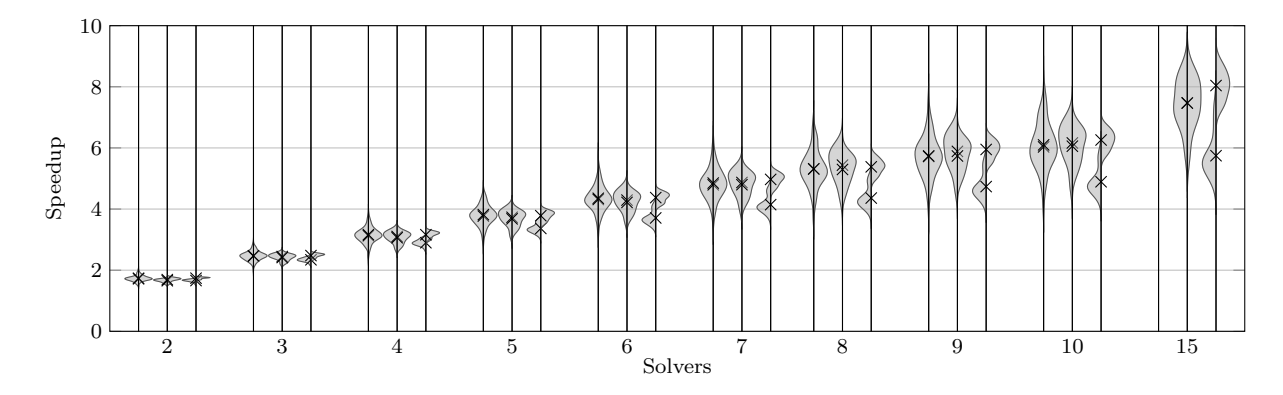
other hand, the core optimization procedure exhibits a sub-linear, but steady, speedup increase that becomes increasingly marginal as we move to a higher number of solvers.

Ideally, the core optimization procedure should also scale linearly with the number of solvers, especially on the largest I instances. However, there are several factors that could contribute to this sub-linear behavior. First, as described in Section 6.2, the probability of generating a conflicting change grows steadily as the number of solvers increases, and whenever a change is discarded, an additional core optimization iteration must be performed. Moreover, hardware characteristics such as CPU-level cache contention among threads begin to play an important role, especially for a complex procedure such as the core optimization, where every solver manages and uses considerably large data structures. Finally, while instance preprocessing does only need very limited synchronization, core optimization requires acquiring locks when interacting with the dispatcher and solver queues, and despite this being minimal, it adds up to the other factors.

Figure 6 shows the overall FILO2 x speedup distribution obtained by standard and long runs. The graph shows that the algorithm speedup is similar across different datasets, except when solving $\mathbb I$ instances with standard runs. In this case, the 6% sequential processing still happening significantly reduces the overall algorithm speedup.

Finally, Figure 7 provides some insight into the algorithm speedup with respect to some instance characteristics. In particular, the chart shows that the speedup does not depend on the instance size but rather on

Figure 6: Speedup distribution obtained by FILO2^x while varying the number of solvers. Each group refers from left-to-right to the \mathbb{X} , \mathbb{B} , and \mathbb{I} datasets. In addition, within every group, each plot represents the speedup obtained by regular (left) and long (right) runs. Average values are denoted by the \times symbol. Results for the \mathbb{X} dataset with 15 solvers are not available due to the high contention among solvers; see 6.2.



the estimated number of routes required by a solution. The more routes, the higher the expected speedup. This is especially visible for the \mathbb{X} and \mathbb{B} instances given the relatively small number of routes they require compared to the \mathbb{I} instances, where the speedup differences are less pronounced. As will be illustrated in Section 6.2, this behavior is closely linked to the likelihood of generating infeasible changes when few routes are available.

6.2. Infeasible/Inapplicable Changes

The main characteristic of FILO2 x consists in allowing solvers to freely optimize localized solution portions without imposing any centralized guidance or rigid boundaries. As a result, several solvers may ultimately optimize overlapping areas. In general, the resulting changes can still produce CVRP-feasible solutions depending on when they were generated and the order in which they are sent to the dispatcher.

The asynchronous nature of $FILO2^x$ makes every solver have a reference solution that belongs to the same shared search trajectory but may be at a different point. As a result, it is very likely that all solvers will generate changes using slightly different reference solutions. In general, incorporating a change that was generated on a slightly different solution can still produce a CVRP-feasible solution depending on the area affected by the change and on the entity of the difference.

However, the combination of overlapping optimization on non-synchronized reference solutions has a high probability of generating changes producing infeasible solutions. This issue is mitigated by re-validating the feasibility of candidate changes received during the synchronization stage. Figure 8 shows the fraction of candidate changes that when applied to a solver reference solution during the synchronization stage generate an infeasible solution. Note that because every solver traverses the same search trajectory, they will all encounter the same feasible and infeasible solutions.

For the X, the median infeasibility frequency increases to up to 20% when employing 10 solvers, with peaks well above twice that value for some runs of instances X-n157-k13, X-n162-k11, X-n411-k19, and X-n308-k13. For the larger B instances, the infeasibility frequency shows a more compact set of values around the

Figure 7: Median speedup averaged across parallel variants with 2 to 10 solvers. Dots represent instances. The y-axis denoted as Routes[†] is defined as the sum of customer demands over the vehicle capacity, and provides a rough estimate on the number of routes required by a solution. Note that for better visualization, both axis for the \mathbb{X} chart are logarithmic.

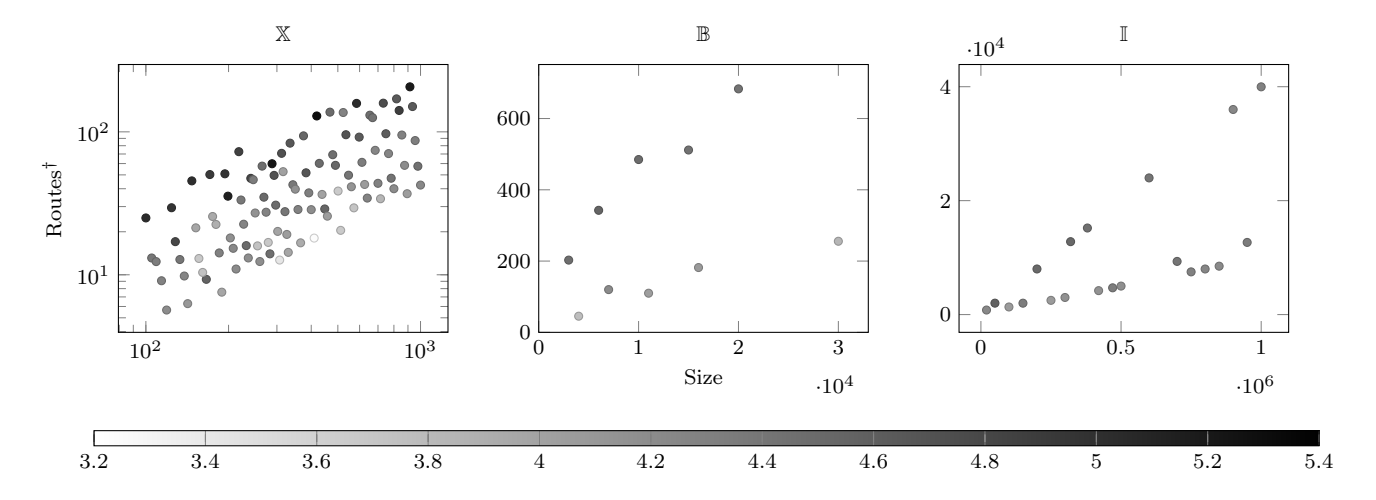
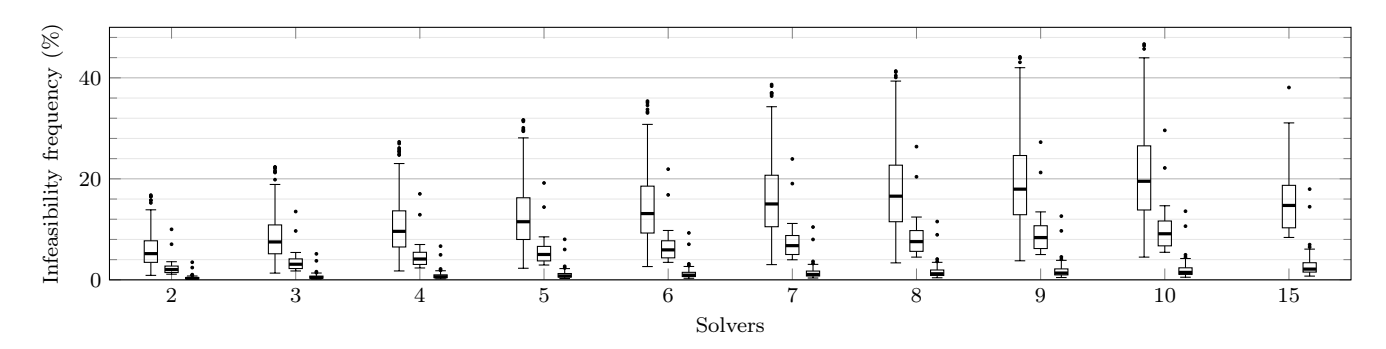


Figure 8: Percentage of candidate changes leading to infeasible solutions for different instances and run configurations. Each box plot group refers from left-to-right to the \mathbb{X} , \mathbb{B} , and \mathbb{I} datasets. The results for 15 solvers only refer to the \mathbb{B} and \mathbb{I} instances due to the high contention among solvers when solving the \mathbb{X} instances.



median that reaches the value of 8% when using 10 solvers, with Leuven2 as an outlier during both standard and long runs. The variability among infeasibility frequency values grows considerably when employing 15 solvers. Finally, the I dataset shows a more consistent behavior across the considered number of solvers, with a median infeasibility frequency around 2% when using 15 solvers. Instance Valle-D-Aosta shows a considerably higher number of infeasibility frequency during both standard and long runs.

As better illustrated in Figure 9, all the instances mentioned above share the common characteristic of having a small number of routes. This chart is mostly a specular copy of the speedup chart of Figure 7. Indeed, for every discarded change, the algorithm requires an additional core optimization iteration to reach the required termination criterion, with a clear negative effect on overall speedup. The likelihood of generating changes leading to infeasible solutions is closely related to the number of routes that make up a solution. The fewer the routes, the higher the chance that solvers optimize an overlapping set of routes, which makes generating a resulting CVRP-feasible solution from these independent optimizations extremely challenging.

Figure 9: Median change infeasibility frequency averaged across parallel version with 2 to 10 solvers. Dots represent instances. The y-axis denoted as Routes[†] is defined as the sum of customer demands over the vehicle capacity, and provides a rough estimate on the number of routes required by a solution. Note that for better visualization, both axis for the $\mathbb X$ chart are logarithmic.

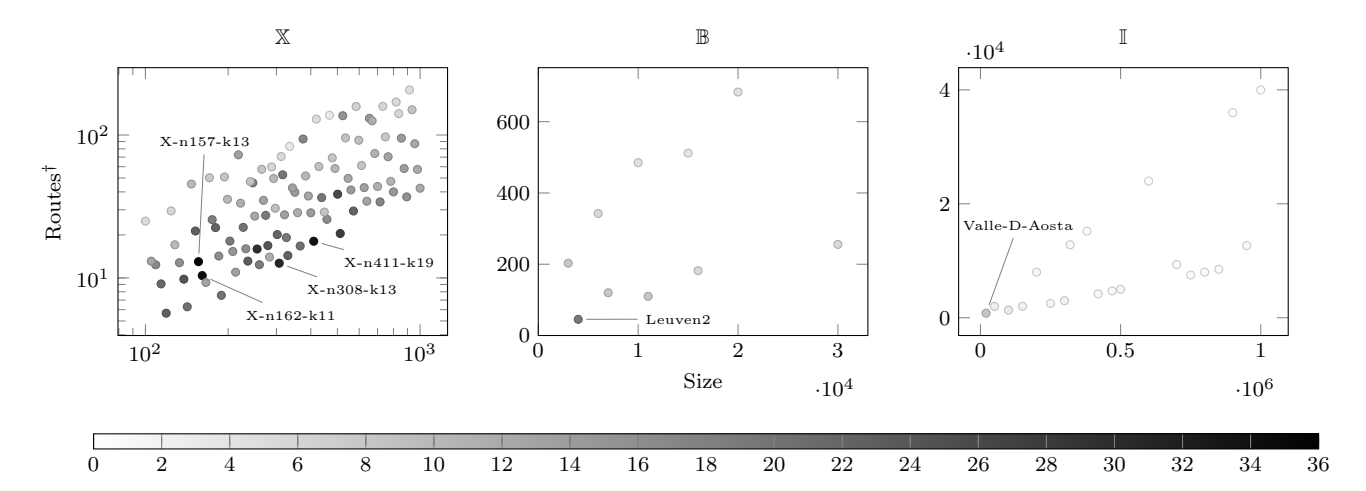
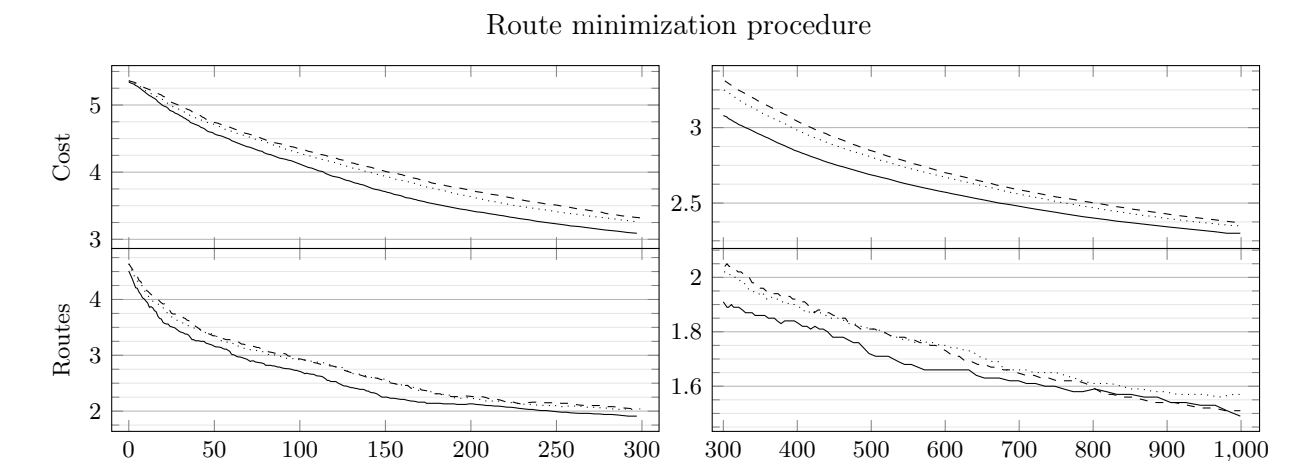


Figure 10: Search trajectory of the best-quality solution found during $\Delta_{RM} = 1000$ route minimization procedure iterations, averaged across datasets. Note that usually the route minimization procedure ends whenever the required number of routes is achieved. However, for the purpose of the analysis we performed exactly Δ_{RM} iterations, regardless of the previously mentioned termination criterion. The Cost label denotes the average solution cost gap with respect to the best known solution. The Routes label denotes the average route gap with respect to the greedy estimate employed to determine whether to run the route minimization procedure. The continuous, dotted, and dashed lines refer to the sequential, and parallel versions with 5 and 10 solvers, respectively. The graph is split in 0-300 and 300-999 iterations for better visibility.



Iterations

6.3. Route Minimization Procedure Parallelization

In principle, the route minimization procedure could be parallelized using the same schema applied for the core optimization procedure. However, as shown in Figure 10, there is a significant degradation in the quality of the solutions obtained that increases with the number of solvers employed. For the largest instances, this difference remains even after the application of the core optimization procedure, causing a statistically significant difference between the final results of the sequential algorithm compared to the parallel versions employing several solvers.

The motivation behind such a reduction in solution quality is unclear and likely depends on the specifics of the route minimization procedure (see Algorithm 2). In particular, the key differences with the core optimization procedure are in the recreate step and in the neighbor acceptance criteria. The recreate step

Figure 11: Percentage of candidate changes leading to infeasible solutions during the parallel route minimization procedure. Each box plot group refers from left-to-right to the \mathbb{X} , \mathbb{B} , and \mathbb{I} datasets.

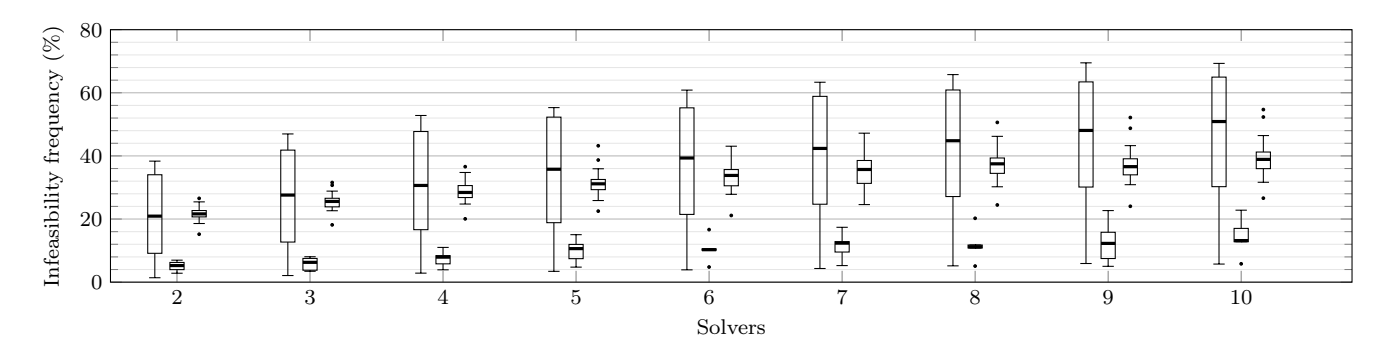
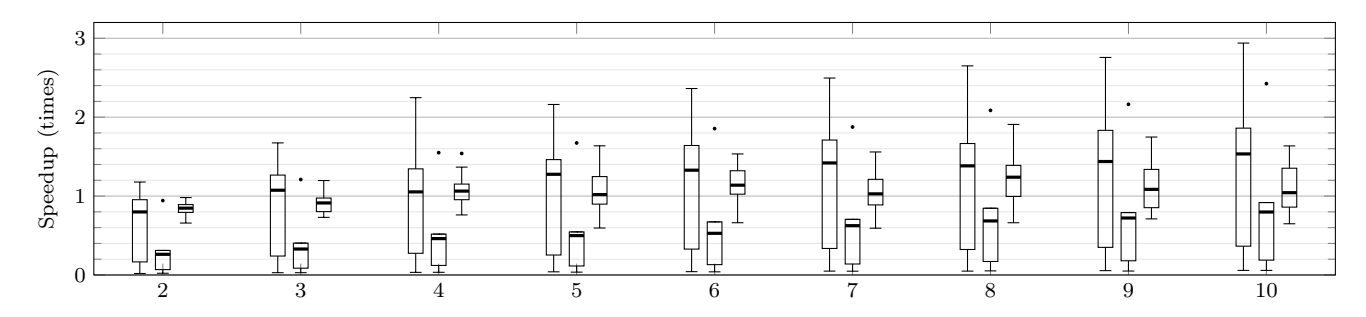


Figure 12: Speedup of the parallel route minimization procedure. Each box plot group refers from left-to-right to the \mathbb{X} , \mathbb{B} , and \mathbb{I} datasets.



can probabilistically leave some customers unserved for multiple iterations (lines 13 - 17), while a generated neighbor solution is only accepted when improving and is reverted to the best solution found otherwise (lines 22 - 25, 27). Most probably, these differences make the parallel versions less effective, even though we could not pinpoint the specific cause.

Indeed, also Figure 11 shows a surprisingly high chance of generating candidate changes leading to infeasible solutions, with a peak well above 60% for some X instances. This is most likely due to the strict reset-to-best rule (line 27) which, when applied, can have a global effect on the reference solution, greatly enhancing the chance of invalidating any change produced on previous reference solutions. As shown in Figure 12, this has a hugely negative effect on the procedure speedup, which even makes the parallel version slower than the sequential version for some configurations.

Because of these issues and the short computing time the sequential route minimization is anyway taking even for the largest instances (see Tables A.19 and A.20), we decided not to invest more in its parallelization.

6.4. Synchronization and Generation Time

Synchronization is the key stage that allows solvers to incorporate changes generated by other solvers on potentially different reference solutions. It is the main additional step that the parallel version performs compared to the sequential algorithm, where synchronization and generation coexist into one single cohesive step. For the parallel approach to be successful, it is crucial that the synchronization overhead, which includes re-validating a received change, is still negligible with respect to the execution of the generation stage.

As can be seen in Table 3, the generation time takes most of the total time of the core optimization procedure, with the local search step taking more than 86% of it. The synchronization time starts becoming relevant as the instances get larger and the number of solvers increase.

Table 3: Fraction of core optimization procedure spent doing the synchronization and generation stages.

	Solvers	2	3	4	5	6	7	8	9	10
\mathbb{X}	Synchronization Generation	$0.04 \\ 0.95$	$0.06 \\ 0.94$	$0.08 \\ 0.92$	0.10 0.90	0.11 0.88	$0.13 \\ 0.86$	$0.15 \\ 0.85$	$0.17 \\ 0.82$	0.19 0.80
\mathbb{B}	Synchronization Generation	$0.05 \\ 0.95$	$0.07 \\ 0.93$	$0.09 \\ 0.91$	$0.11 \\ 0.89$	$0.12 \\ 0.87$	$0.14 \\ 0.85$	$0.16 \\ 0.84$	$0.18 \\ 0.82$	0.19 0.80
I	Synchronization Generation	0.09 0.90	0.13 0.86	$0.16 \\ 0.82$	0.19 0.78	$0.22 \\ 0.75$	$0.25 \\ 0.72$	$0.27 \\ 0.69$	$0.30 \\ 0.67$	0.32 0.64

7. Conclusions

In this paper, we introduced a schema for parallelizing iterations of optimization approaches that scope their actions on a localized solution portion, without the need for decomposition or rigid boundaries. This schema is applied to FILO2, an already extremely efficient algorithm capable of scaling to instances with several hundreds of thousands of vertices. The resulting FILO2 x algorithm can be classified as an Independent Multi-Search (IMS/p-Control) approach with an indirect data exchange strategy, through the use of message queues, and an asynchronous cooperative optimization process. The FILO2 x algorithm maintains the effectiveness of FILO2, producing state-of-the-art results on datasets from the literature, but in a fraction of time. Interestingly, the approach can be applied to small instances with a few hundred vertices still obtaining good speedups. In general, the higher the number of routes used by a solution, the better the speedup, as this reduces the likelihood of generating changes leading to infeasible solutions.

Appendix A. Additional Computational Details

In the following, Appendix A.1, Appendix A.2, and Appendix A.3 provide additional computational details for the \mathbb{X} , \mathbb{B} , and \mathbb{I} datasets, respectively. We also provide statistical validation of the algorithm results to better understand whether there are statistically significant differences between the behavior of FILO2^x and FILO2. In particular, as in Accorsi and Vigo (2024), we perform a one-tailed Wilcoxon signed rank test (see Wilcoxon (1945)) where the null and alternative hypotheses H_0 and H_1 , respectively, are defined as follows.

 H_0 : AVERAGECOST(FILO2^x) = AVERAGECOST(FILO2)

 $H_1: AVERAGECOST(FILO2^x) > AVERAGECOST(FILO2)$

A hypothesis is rejected if its associated p-value is smaller than a significance level α . When the null hypothesis H_0 is not rejected, the average results of FILO2^x are not statistically different from those obtained by FILO2. In contrast, rejecting H_0 means that the average results obtained by the algorithms are statistically different. The alternative hypothesis H_1 is thus tested to evaluate whether the average results obtained by FILO2^x are statistically worse than those obtained by FILO2. If H_1 is rejected, FILO2^x performs as well as or better than FILO2.

When multiple comparisons are performed with the same data, the probability of erroneously rejecting a null hypothesis increases. To better control these errors, the significance level α is typically adjusted to lower values. The Bonferroni correction (Dunn (1961)) is a simple method used to adjust α when performing multiple comparisons. In particular, given n comparisons, the significance level is set to α/n . In particular, we set $\alpha = 0.025$ and n = 9, as we are performing one test consisting of two hypotheses for each configuration of the parallel version, using from 2 to 10 solvers. The corrected significance level is therefore $\bar{\alpha} = 0.025/9 = 0.002778$.

Appendix A.1. Computational Details for the X Instances

In the following, we report detailed results for the computations on the X dataset.

- Figure A.13 shows boxplots for the average gaps obtained by the approaches.
- Table A.4 shows the result of the one-tailed Wilcoxon signed rank test.
- Tables A.5 and A.6 report the computing time for the main algorithm procedures.
- Tables A.7 A.9 show the average gap for each instance in the dataset.
- \bullet Tables A.10 A.12 show the average speedup for each instance in the dataset.

Figure A.13: Average gaps obtained by FILO2 and FILO2 x (denoted by the number of solvers) on the $\mathbb X$ dataset when executing the standard (top) and long (bottom) versions. The median value is shown in the middle of each boxplot.

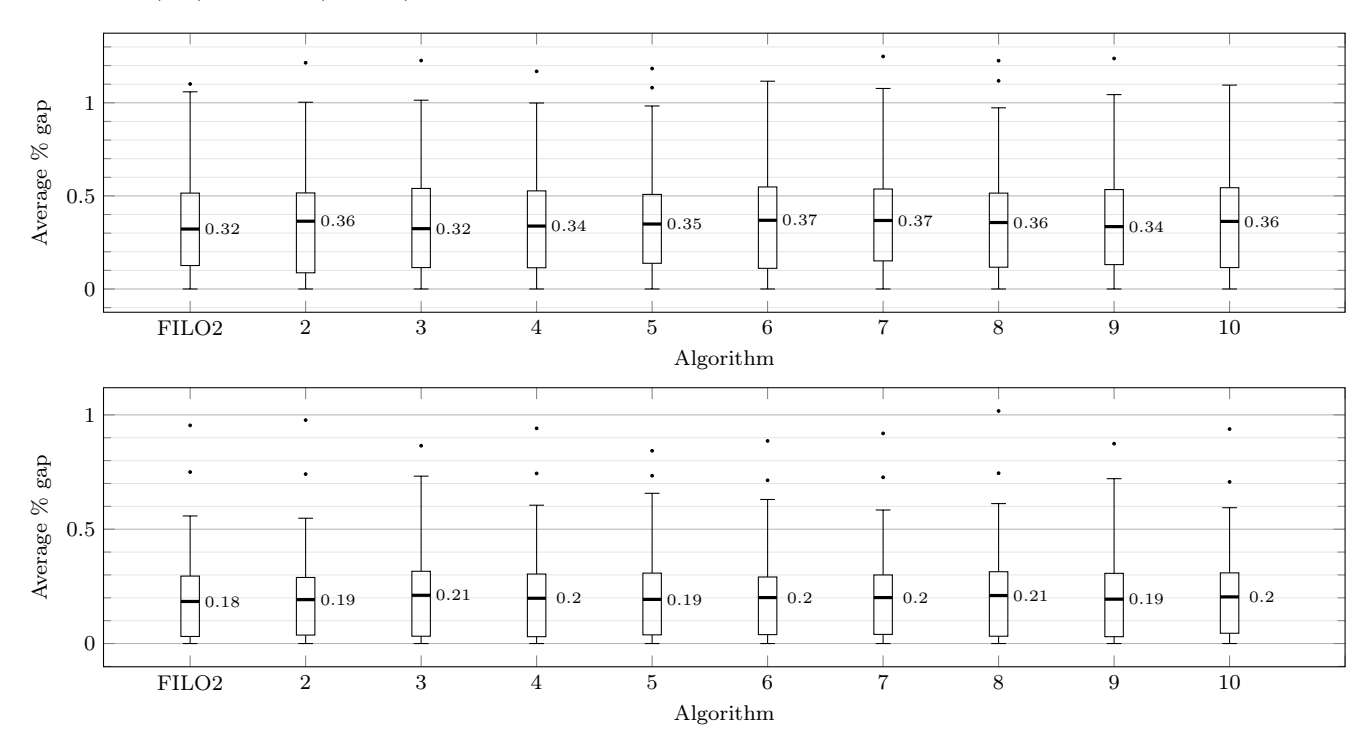


Table A.4: Computations on the \mathbb{X} dataset: p-values for FILO2 x vs FILO2 on the left and FILO2 x (long) vs FILO2 (long) on the right.

p-values in bold are associated with rejected hypothesis when $\bar{\alpha}=0.002778.$

The last row of each group contains a p-value interpretation. In particular, FILO2 x is not statistically different from FILO2 when H_0 cannot be rejected (Similar), FILO2 x is statistically better when both H_0 and H_1 are rejected (Better), and, finally, FILO2 x is statistically worse when H_0 is rejected and H_1 is not rejected (Worse).

	$\mathrm{FILO2}^x$ vs FII	LO2	$FILO2^x$ (long) vs FII	LO2 (long)
Solvers	$H_0 \ / \ H_1$	Outcome	$H_0 \ / \ H_1$	Outcome
2	$0.636031 \ / \ 0.318015$	Similar	$0.686502 \; / \; 0.343251$	Similar
3	$0.861598 \ / \ 0.430799$	Similar	$0.986721 \ / \ 0.493360$	Similar
4	$0.204705 \; / \; 0.897648$	Similar	$0.918803 \ / \ 0.540598$	Similar
5	$0.400299 \ / \ 0.799850$	Similar	$0.748675 \ / \ 0.374337$	Similar
6	$0.093292 \ / \ 0.953354$	Similar	$0.702061 \ / \ 0.351031$	Similar
7	$0.019983 \ / \ 0.990009$	Similar	$0.352392 \ / \ 0.823804$	Similar
8	$0.354791 \ / \ 0.822604$	Similar	$0.184298 \ / \ 0.907851$	Similar
9	$0.146985 \ / \ 0.926507$	Similar	$0.434540 \ / \ 0.782730$	Similar
10	$0.022747 \; / \; 0.988626$	Similar	$0.112887 \; / \; 0.943557$	Similar

Table A.5: Computing time in seconds for the main algorithm FILO2 and FILO2 x procedures when solving the $\mathbb X$ dataset.

					FIL	$O2^x$				
	FILO2	2	3	4	5	6	7	8	9	10
Instance preprocessing	0.03	0.02	0.02	0.01	0.01	0.01	0.01	0.01	0.01	0.01
Construction phase	0.00	0.00	0.00	0.00	0.00	0.00	0.00	0.00	0.00	0.00
Greedy route estimation	0.00	0.00	0.00	0.00	0.00	0.00	0.00	0.00	0.00	0.00
Move generators initialization	0.00	0.00	0.00	0.00	0.00	0.00	0.00	0.00	0.00	0.00
Route minimization procedure	0.25	0.26	0.27	0.27	0.27	0.27	0.27	0.27	0.27	0.27
Core optimization procedure	66.91	39.13	27.46	21.66	18.01	15.80	14.20	12.89	12.01	11.39

Table A.6: Computing time in seconds for the main algorithm FILO2 (long) and FILO2 x (long) procedures when solving the $\mathbb X$ dataset.

					FIL	$O2^x$				
	FILO2	2	3	4	5	6	7	8	9	10
Instance preprocessing	0.03	0.02	0.01	0.01	0.01	0.01	0.01	0.01	0.01	0.01
Construction phase	0.00	0.00	0.00	0.00	0.00	0.00	0.00	0.00	0.00	0.00
Greedy route estimation	0.00	0.00	0.00	0.00	0.00	0.00	0.00	0.00	0.00	0.00
Move generators initialization	0.00	0.00	0.00	0.00	0.00	0.00	0.00	0.00	0.00	0.00
Route minimization procedure	0.25	0.26	0.27	0.27	0.27	0.27	0.27	0.27	0.27	0.27
Core optimization procedure	704.80	407.10	285.79	224.22	186.18	163.57	146.77	134.13	124.27	117.18

Table A.7: Average gap on small-sized $\mathbb X$ instances.

							$FILO2^x$	2^x				FILO2				FII	$FILO2^x (long)$	ong)			
Instance	BKS	FILO2	2	3	4	1 5	9 9	2	∞	6	10	(long)	2	3	4	ಬ	9	2	∞	6	10
X-n101-k25	27591	0.00	0.00	0.00	0.00	_		_	0.00	0.03	0.00	0.00	0.00	0.00	0.00	0.00	0.00	0.00	0.00	0.00	0.00
X-n106-k14	26362	90.0	0.06	0.05	0.03	_		_	0.06	0.06	0.05	0.00	0.00	0.01	0.01	0.01	0.00	0.00	0.01	0.00	0.01
X-n110-k13	14971	0.00	0.00	0.00	0.00	_		_	0.00	0.00	0.00	0.00	0.00	0.00	0.00	0.00	0.00	0.00	0.00	0.00	0.00
X-n115-k10	12747	0.00	0.00	0.00	0.00	_		_	0.00	0.00	0.00	0.00	0.00	0.00	0.00	0.00	0.00	0.00	0.00	0.00	0.00
X-n120-k6	13332	0.00	0.00	0.00	0.00	_	0.00	_	0.00	0.00	0.00	0.00	0.00	0.00	0.00	0.00	0.00	0.00	0.00	0.00	0.00
X-n125-k30	55539	0.51	0.61	0.65	0.69	9 0.78	3 0.55	_	0.51	0.53	0.57	0.22	0.13	0.32	0.16	0.11	0.05	0.32	0.22	0.19	90.0
X-n129-k18	28940	0.13	0.05	0.09	0.05	5 0.04	90.0	_	0.07	0.05	0.05	0.03	0.04	0.03	0.03	0.04	0.03	0.02	0.02	0.03	0.04
X-n134-k13	10916	0.12	0.13	0.16	0.13	_	0.15	0.14	0.16	0.15	0.16	0.02	0.06	0.03	0.02	0.05	0.07	0.07	0.05	0.04	0.05
X-n139-k10	13590	0.00	0.00	0.00	0.00	0.00	0.00	_	0.00	0.00	0.00	0.00	0.00	0.00	0.00	0.00	0.00	0.00	0.00	0.00	0.00
X-n143-k7	15700	0.16	0.13	0.17	0.17	7 0.16	0.13	_	0.12	0.17	0.16	0.11	0.10	0.08	0.11	0.13	0.08	0.11	0.13	0.10	0.09
X-n148-k46	43448	0.23	0.15	0.15	0.27		0.20	_	0.11	0.22	0.12	0.00	0.00	0.00	0.00	0.02	0.04	0.01	0.03	0.01	0.07
X-n153-k22	21220	0.18	0.07	0.24	0.29		9.18		0.18	0.26	0.28	0.02	0.02	0.04	0.03	0.02	0.03	0.02	0.04	0.05	0.02
X-n157-k13	16876	0.00	0.00	0.00	0.00		0.00	_	0.00	0.00	0.00	0.00	0.00	0.00	0.00	0.00	0.00	0.00	0.00	0.00	0.00
X-n162-k11	14138	0.17	0.12	0.13	0.11	0.17	0.14	_	0.17	0.19	0.14	0.03	0.03	0.04	0.06	0.04	0.02	0.07	0.05	0.03	0.04
X-n167-k10	20557	0.08	0.07	0.08	0.12		0.10	_	0.10	0.13	0.10	0.00	0.01	0.01	0.02	0.01	0.01	0.01	0.00	0.03	0.01
X-n172-k51	45607	0.01	0.00	0.03	0.01	1 0.04	1 0.01	_	0.00	0.01	0.01	0.00	0.00	0.00	0.00	0.00	0.00	0.00	0.00	0.00	0.00
X-n176-k26	47812	0.52	0.49	0.53	0.77			_	0.47	0.57	0.73	0.08	0.17	0.23	0.22	0.13	0.15	0.18	0.33	0.26	0.24
X-n181-k23	25569	0.01	0.02	0.02	0.02		_	_	0.01	0.03	0.02	0.00	0.00	0.00	0.00	0.00	0.00	0.00	0.00	0.00	0.00
X-n186-k15	24145	0.12	0.08	0.11	0.10			_	0.09	0.08	0.02	0.03	0.04	0.02	0.01	0.03	0.02	0.04	0.03	0.05	0.04
X-n190-k8	16980	0.04	0.07	0.07	0.09		_	_	0.09	0.13	0.06	0.02	0.02	0.01	0.02	0.01	0.02	0.01	0.02	0.02	0.02
X-n195-k51	44225	0.20	0.16	0.19	0.16			_	0.15	0.18	0.26	0.06	0.05	0.04	0.08	0.05	0.09	0.08	0.16	0.09	0.09
X-n200-k36	58578	0.53	0.80	0.70	0.64				0.65	0.76	0.57	0.44	0.35	0.33	0.31	0.39	0.29	0.35	0.42	0.37	0.33
X-n204-k19	19565	0.02	0.02	0.12	0.11			_	0.15	0.12	0.10	0.00	0.00	0.00	0.00	0.00	0.00	0.00	0.01	0.00	0.01
X-n209-k16	30656	0.05	0.07	0.09	0.10			_	0.12	0.07	0.07	0.06	0.05	0.05	0.05	0.06	0.07	0.05	0.05	0.03	0.05
X-n214-k11	10856	0.28	0.27	0.30	0.25	_	0.35	_	0.32	0.28	0.27	0.16	0.19	0.16	0.16	0.15	0.21	0.16	0.17	0.15	0.16
X-n219-k73	117595	0.00	0.00	0.00	0.00			_	0.00	0.00	0.00	0.00	0.00	0.00	0.00	0.00	0.00	0.00	0.00	0.00	0.00
X-n223-k34	40437	0.28	0.37	0.28	0.26	_	_	_	0.31	0.32	0.30	0.17	0.20	0.21	0.20	0.18	0.22	0.19	0.19	0.19	0.19
X-n228-k23	25742	0.18	0.13	0.16	0.22	_		_	0.18	0.15	0.20	0.11	0.16	0.17	0.14	0.11	0.12	0.17	0.11	0.18	0.12
X-n233-k16	19230	0.50	0.40	0.50	0.56			_	0.43	0.44	0.44	0.24	0.31	0.30	0.31	0.30	0.23	0.24	0.34	0.28	0.31
X-n237-k14	27042	0.00	0.03	0.01	0.00	0.03	0.02		0.01	0.00	0.01	0.01	0.01	0.01	0.01	0.01	0.00	0.01	0.00	0.01	0.01
X-n242-k48	82751	0.32	0.25	0.31	0.33	_	_	_	0.27	0.31	0.39	0.11	0.16	0.14	0.14	0.13	0.16	0.13	0.14	0.14	0.16
X-n247-k50	37274	0.79	0.78	0.68	0.75	5 0.79	0.79	0.77	0.71	0.73	0.72	0.50	0.54	0.44	0.50	0.50	0.41	0.32	0.45	0.59	0.50
Mean		0.17	0.17	0.18	0.20	0.18	3 0.18	3 0.20	0.17	0.19	0.18	0.08	0.08	0.08	0.08	0.08	0.07	0.08	0.00	0.09	0.08

Table A.8: Average gap on medium-sized $\mathbb X$ instances.

							$FILO2^x$	a				FILO2				FII	$FILO2^x$ (long)	long)			
Instance	BKS	FILO2	2	8	4	ro	9	7	∞	6	10	(long)	2	က	4	ಸರ	9	7	∞	6	10
X-n251-k28	38684	0.30	0.39	0.32	0.36	0.31	0.38	0.31	0.39	0.38	0.32	0.24	0.23	0.26	0.23	0.23	0.27	0.28	0.26	0.24	0.25
X-n256-k16	18839	0.22	0.22	0.22	0.22	0.22	0.22	0.22	0.22	0.22	0.22	0.22	0.22	0.22	0.22	0.22	0.22	0.22	0.22	0.22	0.22
X-n261-k13	26558	0.33	0.36	0.39	0.33	0.40	0.30	0.41	0.37	0.39	0.39	0.25	0.24	0.31	0.28	0.29	0.26	0.28	0.25	0.19	0.31
X-n266-k58	75478	0.46	0.45	0.41	0.48	0.47	0.48	0.42	0.40	0.46	0.45	0.29	0.35	0.35	0.35	0.35	0.34		0.33	0.34	0.32
X-n270-k35	35291	0.17	0.21	0.23	0.25	0.24	0.23	0.22	0.22	0.26	0.26	0.17	0.18	0.17	0.18	0.15	0.13		0.13	0.18	0.20
X-n275-k28	21245	0.03	0.07	0.03	0.03	0.02	0.02	0.05	0.05	0.06	0.00	0.00	0.00	0.00	0.00	0.00	0.02	0.00	0.00	0.00	0.00
X-n280-k17	33503	0.35	0.40	0.30	0.35	0.44	0.39	0.40	0.34	0.29	0.42	0.22	0.28	0.31	0.29	0.31	0.24	0.25	0.22	0.25	0.22
X-n284-k15	20215	0.44	0.52	0.58	0.39	0.39	0.38	0.49	0.32	0.43	0.63	0.24	0.23	0.24	0.20	0.22	0.26	0.24	0.27	0.25	0.24
X-n289-k60	95151	0.59	0.55	0.60	0.52	0.53	0.56	0.61	0.00	0.57	0.62	0.43	0.41	0.42	0.39	0.36	0.39	0.36	0.38	0.40	0.37
X-n294-k50	47161	0.32	0.31	0.32	0.28	0.30	0.36	0.30	0.32	0.32	0.29	0.20	0.21	0.21	0.24	0.19	0.21	0.20	0.23	0.26	0.20
X-n298-k31	34231	0.24	0.25	0.18	0.27	0.18	0.29	0.30	0.34	0.25	0.33	0.19	0.17	0.15	0.14	0.17	0.17	0.18	0.17	0.20	0.13
X-n303-k21	21736	0.44	0.47	0.43	0.51	0.46	0.48	0.47	0.51	0.51	0.41	0.31	0.30	0.33	0.31	0.31	0.34	0.30	0.29	0.31	0.31
X-n308-k13	25859	0.73	0.48	0.75	1.00	1.08	0.74	0.91	1.12	0.91	0.79	0.29	0.25	0.53	0.37	0.66	0.36	0.34	0.23	0.34	0.41
X-n313-k71	94043	0.51	0.52	0.53	0.57	0.52	0.55	0.59	0.46	0.48	0.58	0.28	0.28	0.35	0.27	0.26	0.29	0.27	0.27	0.35	0.33
X-n317-k53	78355	0.01	0.00	0.00	0.01	0.01	0.01	0.01	0.01	0.00	0.00	0.00	0.00	0.00	0.00	0.00	0.00	0.00	0.00	0.00	0.00
X-n322-k28	29834	0.49	0.43	0.43	0.41	0.37	0.42	0.50	0.40	0.49	0.43	0.29	0.21	0.38	0.31	0.26	0.32	0.34	0.35	0.31	0.31
X-n327-k20	27532	0.50	0.40	0.54	0.40	0.43	0.53	0.42	0.47	0.43	0.46	0.28	0.31	0.25	0.30	0.26	0.29	0.29	0.30	0.28	0.29
X-n331-k15	31102	0.03	0.06	0.01	0.03	0.01	0.04	0.05	0.03	0.08	0.08	0.01	0.01	0.01	0.00	0.00	0.01	0.02	0.01	0.00	0.01
X-n336-k84	139111	0.56	0.51	0.54	0.56	0.52	0.58	0.58	0.58	0.61	0.53	0.35	0.30	0.35	0.34	0.34	0.31	0.32	0.31	0.30	0.27
X-n344-k43	42050	0.52	0.56	0.55	0.48	0.55	0.55	0.54	0.54	0.50	0.53	0.34	0.27	0.30	0.37	0.40	0.29	0.32	0.35	0.34	0.34
X-n351-k40	25896	0.62	0.60	0.62	0.63	0.69	0.51	0.00	0.61	0.59	0.67	0.42	0.42	0.39	0.43	0.39	0.45	0.46	0.44	0.47	0.42
X-n359-k29	51505	0.41	0.44	0.41	0.43	0.36	0.44	0.45	0.41	0.44	0.46	0.19	0.20	0.16	0.18	0.20	0.20	0.20	0.22	0.17	0.20
X-n367-k17	22814	0.19	0.06	0.10	0.14	0.15	0.08	0.18	0.16	0.12	0.23	0.03	0.04	0.03	0.04	0.02	0.04	0.02	0.02	0.02	0.04
X-n376-k94	147713	0.01	0.01	0.01	0.01	0.01	0.01	0.01	0.01	0.01	0.01	0.01	0.00	0.00	0.00	0.00	0.00	0.00	0.01	0.00	0.00
X-n384-k52	65928	0.33	0.41	0.39	0.45	0.36	0.38	0.39	0.36	0.41	0.41	0.31	0.28	0.27	0.26	0.26	0.27	0.26	0.28	0.27	0.25
X-n393-k38	38260	0.17	0.19	0.23	0.32	0.26	0.27	0.22	0.19	0.20	0.20	0.00	0.11	0.09	0.12	0.09	0.09	0.10	0.08	0.13	0.12
X-n401-k29	66154	0.24	0.26	0.23	0.22	0.27	0.24	0.23	0.24	0.23	0.22	0.17	0.14	0.13	0.13	0.12	0.14	0.15	0.15	0.13	0.13
X-n411-k19	19712	0.45	0.36	0.55	0.44	0.40	0.40	0.45	0.43	0.36	0.47	0.33	0.33	0.34	0.34	0.32	0.38	0.32	0.32	0.32	0.32
X-n420-k130	107798	0.26	0.27	0.22	0.25	0.27	0.31	0.26	0.26	0.26	0.23	0.17	0.15	0.13	0.17	0.16	0.12	0.17	0.14	0.13	0.13
X-n429-k61	65449	0.40	0.38	0.36	0.34	0.39	0.40	0.44	0.40	0.35	0.43	0.19	0.25	0.18	0.22	0.23	0.21	0.24	0.22	0.21	0.22
X-n439-k37	36391	0.05	0.09	0.06	0.08	0.05	0.10	0.10	0.06	0.11	0.06	0.03	0.03	0.01	0.01	0.04	0.01	0.04	0.03	0.02	0.01
X-n449-k29	55233	0.62	0.60	0.64	0.69	0.68	0.70	0.64	0.59	0.72	0.64	0.36	0.32	0.31	0.30	0.32	0.31	0.31	0.28	0.32	0.35
X-n459-k26	24139	0.29	0.33	0.29	0.39	0.29	0.38	0.41	0.45	0.30	0.36	0.21	0.25	0.23	0.17	0.25	0.29	0.21	0.23	0.27	0.24
X-n469-k138	221824	1.06	1.00	1.01	0.99	0.98	0.96	0.97	0.97	1.04	0.94	0.54	0.55	0.59	0.60	0.62	0.60	0.58	0.55	0.63	0.57
X-n480-k70	89449	0.35	0.38	0.39	0.35	0.36	0.30	0.38	0.36	0.35	0.36	0.18	0.17	0.17	0.16	0.22	0.15	0.19	0.17	0.22	0.17
X-n491-k59	66483	0.61	0.49	0.48	0.50	0.48	0.43	0.54	0.51	0.53	0.53	0.30	0.30	0.29	0.32	0.33	0.28	0.30	0.37	0.32	0.30
Mean		0.37	0.36	0.37	0.38	0.37	0.37	0.39	0.38	0.38	0.39	0.23	0.22	0.24	0.23	0.24	0.23	0.23	0.22	0.23	0.23

Table A.9: Average gap on large-sized $\mathbb X$ instances.

							$\overline{\text{FILO2}^x}$	<i>x</i>				FILO2				FIL($FILO2^x (long)$	ng)			
Instance	BKS	FIL02	2	3	4	2	9	7	8	6	10	(long)	2	3	4	2	9	2	8	6	10
X-n502-k39	69226	0.04	0.04	0.03	90.0	0.05	0.06	0.06	0.05	0.06	0.04	0.03	0.03	0.03	0.03	0.04	0.04	0.04	0.03	0.03	0.05
X-n513-k21	24201	0.32	0.25	0.35	0.26	0.35	0.28	0.27	0.24	0.31	0.27	0.08	0.08	0.13	0.21	0.14	0.09	0.19	0.00	0.12	0.13
X-n524-k153	154593	0.41	0.48	0.41	0.51	0.50	0.56	0.53	0.52	0.57	0.53	0.15	0.19	0.27	0.30	0.23	0.27	0.28	0.38	0.31	0.25
X-n536-k96	94846	0.86	0.82	0.83	0.87	0.87	0.84	0.83	0.87	0.84	0.88	0.75	0.74	0.73	0.74	0.73	0.71	0.73	0.74	0.72	0.71
X-n548-k50	86700	0.12	0.09	0.10	0.08	0.10	0.05	0.11	0.07	0.09	0.00	0.04	0.02	0.04	0.02	0.05	0.04	0.04	0.03	0.03	0.05
X-n561-k42	42717	0.37	0.38	0.35	0.43	0.37	0.38	0.38	0.42	0.36	0.43	0.21	0.24	0.22	0.26	0.18	0.18	0.21	0.21	0.27	0.24
X-n573-k30	50673	0.35	0.45	0.51	0.37	0.40	0.47	0.45	0.39	0.40	0.46	0.24	0.19	0.21	0.21	0.20	0.26	0.20	0.19	0.22	0.25
X-n586-k159	190316	09.0	0.68	0.63	0.60	0.66	0.63	0.65	0.64	0.62	0.62	0.41	0.42	0.44	0.38	0.34	0.38	0.36	0.39	0.36	0.38
X-n599-k92	108451	0.45	0.39	0.48	0.41	0.42	0.50	0.41	0.36	0.34	0.47	0.27	0.30	0.25	0.28	0.27	0.23	0.29	0.25	0.28	0.28
X-n613-k62	59535	0.71	0.68	0.64	0.61	0.64	0.66	0.75	0.69	89.0	0.64	0.32	0.36	0.36	0.35	0.32	0.34	0.41	0.36	0.30	0.34
X-n627-k43	62164	0.34	0.38	0.32	0.32	0.35	0.36	0.32	0.36	0.34	0.39	0.22	0.21	0.21	0.23	0.20	0.20	0.24	0.25	0.22	0.23
X-n641-k35	63682	0.32	0.41	0.35	0.40	0.39	0.45	0.37	0.41	0.34	0.36	0.18	0.21	0.26	0.21	0.25	0.21	0.28	0.24	0.18	0.22
X-n655-k131	106780	0.04	0.03	0.04	0.03	0.03	0.04	0.04	0.04	0.04	0.04	0.02	0.02	0.02	0.03	0.02	0.02	0.02	0.02	0.02	0.02
X-n670-k130	146332	1.10	1.21	1.23	1.17	1.18	1.12	1.25	1.23	1.24	1.10	0.95	0.98	0.86	0.94	0.84	0.89	0.92	1.02	0.87	0.94
X-n685-k75	68205	0.64	0.60	0.55	0.64	0.61	0.64	0.60	0.58	0.55	0.58	0.36	0.43	0.42	0.46	0.43	0.37	0.38	0.44	0.43	0.43
X-n701-k44	81923	0.46	0.47	0.45	0.46	0.45	0.47	0.43	0.48	0.47	0.41	0.13	0.17	0.21	0.20	0.20	0.19	0.17	0.21	0.17	0.20
X-n716-k35	43373	0.64	0.61	0.73	0.73	0.64	0.72	0.62	0.72	0.64	0.69	0.33	0.28	0.31	0.24	0.29	0.28	0.30	0.34	0.28	0.28
X-n733-k159	136187	0.31	0.34	0.31	0.33	0.36	0.39	0.36	0.36	0.33	0.35	0.20	0.20	0.21	0.19	0.21	0.21	0.20	0.21	0.22	0.22
X-n749-k98	77269	0.72	0.71	0.71	0.72	0.73	0.69	0.74	0.73	0.74	0.77	0.46	0.43	0.43	0.48	0.41	0.46	0.42	0.52	0.48	0.48
X-n766-k71	114417	0.69	0.67	0.63	0.65	0.60	0.61	09.0	0.61	0.57	0.66	0.44	0.45	0.36	0.33	0.47	0.38	0.46	0.44	0.42	0.42
X-n783-k48	72386	0.50	0.52	0.52	0.50	0.50	0.56	0.52	0.57	0.63	0.51	0.23	0.26	0.33	0.27	0.30	0.22	0.26	0.30	0.24	0.24
X-n801-k40	73305	0.24	0.22	0.21	0.21	0.22	0.28	0.24	0.24	0.22	0.24	0.13	0.12	0.11	0.12	0.10	0.11	0.15	0.16	0.15	0.14
X-n819-k171	158121	0.78	0.78	0.78	0.76	0.74	0.79	0.83	0.75	0.81	0.80	0.56	0.54	0.54	0.56	0.53	0.54	0.56	0.53	0.53	0.53
X-n837-k142	193737	0.50	0.52	0.48	0.48	0.47	0.47	0.48	0.49	0.47	0.49	0.28	0.27	0.30	0.27	0.31	0.29	0.28	0.27	0.31	0.29
X-n856-k95	88965	0.16	0.17	0.16	0.18	0.17	0.16	0.15	0.17	0.15	0.14	0.11	0.10	0.08	0.07	0.09	0.08	0.08	0.08	0.09	0.08
X-n876-k59	99299	0.46	0.42	0.39	0.46	0.44	0.40	0.47	0.46	0.45	0.43	0.26	0.25	0.25	0.25	0.27	0.22	0.25	0.26	0.25	0.24
X-n895-k37	53860	0.63	0.59	0.62	0.72	0.64	0.61	0.67	0.67	99.0	0.71	0.38	0.38	0.33	0.34	0.36	0.41	0.31	0.32	0.31	0.36
X-n916-k207	329179	0.68	0.68	0.67	0.66	0.67	0.66	0.64	0.68	0.67	0.68	0.41	0.38	0.38	0.40	0.38	0.40	0.37	0.43	0.35	0.36
X-n936-k151	132715	0.90	0.91	0.90	0.95	0.93	0.97	0.96	0.93	1.00	0.96	0.52	0.50	0.47	0.56	0.48	0.63	0.54	0.61	0.59	0.59
X-n957-k87	85465	0.14	0.14	0.13	0.13	0.13	0.11	0.14	0.14	0.16	0.13	0.09	0.07	0.10	0.08	0.09	0.08	80.0	0.09	0.07	0.10
X-n979-k58	118976	0.70	0.67	0.77	0.77	0.76	0.70	0.07	0.65	0.78	0.57	0.15	0.15	0.15	0.14	0.15	0.18	0.16	0.16	0.18	0.16
X-n1001-k43	72355	0.58	0.63	0.65	0.59	0.63	0.69	0.64	0.63	89.0	0.62	0.33	0.29	0.30	0.29	0.21	0.26	0.29	0.31	0.31	0.28
Mean		0.49	0.50	0.50	0.50	0.50	0.51	0.51	0.50	0.51	0.50	0.29	0.29	0.29	0.30	0.28	0.29	0.30	0.31	0.29	0.30

Table A.10: Average speedup on small-sized $\mathbb X$ instances.

Instance																	
)	2	8	4	5 (2 9	∞	6	10	2	3	4	ಬ	9	7	∞	6	10
X-n101-k25 1.	1.75 2.71	71 3.32	2 4.30		2 5.45		6.75	7.06	1.86	2.73	3.55	4.35	5.06	5.67	6.38	96.9	7.31
X-n106-k14 1.	1.73 2.59	59 3.32	2 3.93	34.62	7.	5.88	6.37	7.15	1.71	2.54	3.12	3.82	4.36	5.14	5.46	5.98	6.61
X-n110-k13 1.	1.74 2.51	3.21	1 3.96	6 4.46	7.		6.16	6.34	1.72	2.47	3.15	3.79	4.33	4.82	5.32	5.78	6.11
X-n115-k10 1.	1.73 2.47	17 3.18		7	7,	5.40	5.99	6.11	1.72	2.46	3.14	3.77	4.28	4.76	5.22	5.66	5.97
X-n120-k6 1.	1.73 2.45	15 3.12	2 3.75	7	5 4.68		5.57	5.85	1.71	2.45	3.09	3.69	4.20	4.63	5.11	5.50	5.83
X-n125-k30 1.	1.73 2.57		3 3.59	7	11.5	6.55	6.74	7.03	1.83	2.74	3.67	4.29	5.05	5.11	6.49	6.90	7.70
X-n129-k18 1.	1.83 2.65	35 3.24	4 + 4.31	1 4.94		6.83	7.21	7.30	1.81	2.61	3.36	4.03	4.79	5.42	6.18	6.63	82.9
X-n134-k13 1.	1.73 2.50	3.21		8 4.46		5.48	6.25	6.31	1.74	2.46	3.09	3.85	4.38	4.71	5.41	5.86	90.9
X-n139-k10 1.	1.73 2.48	18 3.14	4 3.78	8 4.28		5.28	5.82	5.99	1.72	2.44	3.08	3.71	4.25	4.68	5.17	5.63	5.99
X-n143-k7 1.		33 3.35	5 3.78	8 4.34		5.34	5.82	5.77	1.77	2.72	3.08	3.62	4.08	4.52	5.18	5.53	5.90
X-n148-k46 1.	1.72 2.57	57 3.07	7 - 4.19	9 4.85	*	5.88	6.08	6.91	1.89	2.73	3.59	4.43	5.04	5.77	6.46	88.9	7.57
X-n153-k22 1.			6 3.34		·		4.81	5.24	1.68	2.30	2.76	3.36	3.96	4.25	4.34	4.76	5.41
X-n157-k13 1.			9 3.11			4.27	4.45	4.68	1.63	2.30	2.82	3.27	3.70	4.00	4.40	4.61	4.90
X-n162-k11 1.	1.59 2.23		1 3.26			4.20	4.59	4.71	1.66	2.29	2.74	3.36	3.75	3.87	4.19	4.68	4.81
X-n167-k10 1.		3.35	5 4.03		1 4.86		6.12	6.99	1.74	2.52	3.40	3.99	4.54	5.13	5.49	5.92	6.22
X-n172-k51 1.			8 4.41	1 - 4.75		5.75	6.52	7.30	1.86	2.68	3.34	4.24	4.93	5.54	6.11	6.56	7.09
X-n176-k26 1.			8 3.94		_		5.21	5.43	1.66	2.45	3.11	3.50	3.94	4.94	4.76	5.13	5.49
X-n181-k23 1.			3 3.40				5.00	5.36	1.65	2.33	2.85	3.47	3.90	4.37	4.67	5.14	5.45
X-n186-k15 1.	1.89 2.50		3 4.14		-		6.15	6.82	1.75	2.39	3.09	3.81	4.28	4.62	5.07	5.46	5.71
					7 4.51		5.18	5.71	1.73	2.43	2.96	3.72	4.00	4.63	4.91	5.31	5.69
X-n195-k51 1.	1.63 2.32			·	*		6.05	6.28	1.93	2.77	3.59	4.48	5.01	5.48	5.86	6.28	7.20
X-n200-k36 1.				•	7	5.69	5.52	6.58	1.92	2.66	3.71	4.26	5.25	5.54	5.77	6.70	7.26
X-n204-k19 1.					7	•	4.96	5.31	1.72	2.42	3.07	3.68	4.19	4.56	5.11	5.42	5.70
X-n209-k16 1.	1.75 2.30		9 3.60	0 - 4.10	0.4.13	5.05	5.56	5.81	1.70	2.58	3.25	3.70	4.25	4.97	5.32	5.78	5.83
X-n214-k11 1.	1.75 2.40	40 3.22	2 3.79	4.		4.88	5.54	2.67	1.81	2.45	3.12	3.94	4.23	4.75	5.28	5.65	5.99
X-n219-k73 1.	1.77 2.62	3.38	8 4.12	2 4.79	9 5.74	90.9	6.59	7.29	1.79	2.64	3.46	4.15	4.84	5.64	6.17	6.75	7.42
X-n223-k34 1.	1.69 2.53	53 3.29	9 3.89	9 4.57	7 4.84	5.68	6.10	96.9	1.69	2.52	3.17	3.84	4.38	4.85	5.41	00.9	6.24
X-n228-k23 1.	1.71 2.37		4 3.52	2 4.19	9 4.41	4.83	5.34	5.39	1.73	2.36	3.17	3.73	4.28	4.43	5.12	5.21	5.76
X-n233-k16 1.	1.54 2.18	18 2.99	9 3.57	7 + 4.13	3 4.22	5.25	5.16	5.51	1.81	2.49	3.37	3.95	4.53	4.89	5.56	5.68	6.44
X-n237-k14 1.	1.61 2.32	32 2.95	5 3.57	7	9 4.63	5.07	5.60	5.53	1.68	2.31	2.96	3.61	4.17	4.41	5.02	5.30	5.38
X-n242-k48 2.	2.01 2.76	3.68	8 4.5′	· ·	5.66		7.36	7.19	1.82	2.53	3.17	4.13	4.81	5.10	5.67	6.63	6.91
X-n247-k50 1.	1.69 2.46	16 3.08	8 3.7	2 + 25	5 4.67	5.29	5.53	5.69	1.78	2.46	3.29	3.92	4.35	5.21	5.36	5.61	6.36
Mean 1.	1.71 2.44	14 3.14	4 3.79	9 4.32	2 4.80	5.34	5.75	60.9	1.75	2.50	3.18	3.83	4.37	4.85	5.33	5.75	6.15

Table A.11: Average speedup on medium-sized $\mathbb X$ instances.

				I	$FILO2^x$								FIL	$FILO2^x (long)$	ng)			
Instance	2	က	4	ಸಂ	9	2	∞	6	10	2	3	4	ಸಂ	9	2	∞	6	10
X-n251-k28	1.75	2.64	3.19	3.84	4.59	5.20	5.29	90.9	6.30	1.67	2.24	3.21	3.91	4.11	4.60	5.46	5.93	5.98
X-n256-k16	1.60	2.32	2.79	3.40	3.84	4.11	4.53	4.97	5.11	1.61	2.18	2.79	3.31	3.72	4.04	4.35	4.72	4.99
X-n261-k13	1.57	2.36	2.99	3.50	4.25	4.35	4.98	5.17	5.59	1.91	2.54	3.15	3.68	4.18	4.44	5.18	5.56	5.81
X-n266-k58	1.76	2.77	3.32	4.04	4.43	5.54	5.85	5.90	6.83	1.75	2.26	3.07	3.72	4.46	4.94	5.23	5.79	6.57
X-n270-k35	1.71	2.39	2.88	3.63	4.22	4.51	5.24	5.35	5.83	1.77	2.59	3.24	4.02	4.52	5.25	5.48	5.99	6.29
X-n275-k28	1.66	2.48	3.09	3.63	4.20	4.75	5.32	5.66	00.9	1.71	2.53	3.13	3.86	4.28	4.81	5.19	5.75	80.9
X-n280-k17	1.64	2.26	2.74	3.16	3.70	3.95	4.53	4.87	4.74	1.55	2.19	2.52	3.15	3.69	4.01	4.40	4.61	4.95
X-n284-k15	1.67	2.47	3.48	3.86	4.74	5.23	5.96	6.14	6.40	1.70	2.47	3.24	3.79	4.42	4.74	5.29	5.70	5.89
X-n289-k60	1.91	2.84	3.50	4.30	4.62	5.42	5.84	6.38	7.38	1.83	2.67	3.71	4.51	5.28	6.27	6.27	6.37	8.08
X-n294-k50	1.89	2.66	3.41	4.02	4.59	5.00	5.42	5.84	6.34	1.72	2.50	3.14	3.99	4.75	5.10	5.48	5.90	6.38
X-n298-k31	1.71	2.59	3.22	3.98	4.42	5.03	5.54	00.9	80.9	1.84	2.53	3.30	3.87	4.49	4.85	5.48	5.88	6.36
X-n303-k21	1.67	2.41	2.92	3.59	3.96	4.28	4.62	4.92	5.19	1.73	2.48	3.02	3.58	4.02	4.29	4.67	4.92	5.07
X-n308-k13	1.53	2.22	2.44	2.90	3.32	3.70	3.77	4.27	4.12	1.60	2.16	2.68	3.18	3.44	3.84	4.13	4.48	4.52
X-n313-k71	1.67	2.50	3.13	3.75	4.59	4.79	5.62	6.12	6.19	1.88	2.47	3.37	4.12	4.75	5.44	6.23	5.88	6.52
X-n317-k53	1.66	2.33	2.88	3.53	3.93	4.44	4.85	5.17	5.50	1.64	2.34	2.97	3.50	4.02	4.43	4.88	5.24	5.59
X-n322-k28	1.78	2.53	3.30	4.06	4.38	4.92	5.69	5.82	6.17	1.83	2.39	3.24	3.85	4.41	4.88	5.13	5.82	5.70
X-n327-k20	1.75	2.33	3.17	3.74	4.10	4.54	5.00	5.62	5.72	1.71	2.48	3.18	3.85	4.05	4.44	5.02	5.53	5.69
X-n331-k15	1.70	2.43	2.95	3.51	4.15	4.59	5.08	5.19	5.65	1.70	2.38	3.06	3.57	3.96	4.31	4.92	5.15	5.64
X-n336-k84	1.91	2.55	3.26	4.16	4.67	5.13	6.14	6.29	98.9	1.84	2.58	3.53	4.01	4.67	5.27	6.28	6.21	7.22
X-n344-k43	1.65	2.33	3.04	3.46	3.93	4.24	4.83	5.21	5.37	1.77	2.49	3.09	3.75	4.43	4.93	4.95	5.38	90.9
X-n351-k40	1.67	2.28	2.91	3.29	4.17	4.39	4.59	5.15	5.26	1.74	2.54	3.16	3.91	4.17	4.55	5.28	5.49	5.78
X-n359-k29	1.73	2.41	3.25	3.86	4.21	4.79	5.15	5.91	6.11	1.74	2.49	3.12	3.82	4.30	4.84	5.10	5.70	6.18
X-n367-k17	1.75	2.40	3.06	3.49	4.04	4.38	4.93	5.11	5.02	1.68	2.30	2.95	3.49	3.92	4.36	4.79	5.04	5.37
X-n376-k94	1.70	2.37	3.02	3.83	4.18	4.83	5.40	5.78	6.16	1.79	2.60	3.30	3.91	4.54	5.18	5.64	6.16	6.59
X-n384-k52	1.64	2.48	3.10	3.79	4.31	4.96	5.41	90.9	6.49	1.74	2.57	3.36	4.10	4.70	5.07	5.70	6.54	6.50
X-n393-k38	1.74	2.51	2.98	3.70	4.25	4.82	5.19	5.51	5.74	1.71	2.49	3.08	3.81	4.33	4.82	5.44	5.67	6.01
X-n401-k29	1.58	2.39	2.96	3.57	4.20	4.60	5.07	5.61	5.78	1.71	2.46	3.07	3.81	4.20	4.50	5.06	5.51	5.98
X-n411-k19	1.50	1.99	2.50	2.97	3.22	3.43	3.72	4.03	4.16	1.48	2.14	2.60	2.94	3.24	3.55	3.81	3.97	4.19
X-n420-k130	1.84	2.58	3.57	3.98	4.53	5.22	5.77	6.55	6.93	1.98	2.82	3.86	4.37	5.40	5.74	6.51	7.31	7.74
X-n429-k61	1.69	2.43	3.35	3.82	4.28	4.68	5.43	5.90	6.24	1.70	2.53	3.29	3.88	4.50	4.85	5.42	80.9	6.34
X-n439-k37	1.71	2.34	3.03	3.76	4.22	4.70	5.10	5.44	5.77	1.69	2.35	2.91	3.54	4.00	4.53	4.98	5.20	5.44
X-n449-k29	1.77	2.47	3.11	3.87	4.39	4.85	5.37	5.70	5.88	1.84	2.50	3.29	4.06	4.55	5.23	5.67	6.02	6.50
X-n459-k26	1.71	2.39	2.98	3.50	3.97	4.45	4.86	5.25	5.60	1.74	2.50	3.11	3.69	4.05	4.64	5.03	5.31	5.64
X-n469-k138	1.98	2.88	3.74	4.38	5.70	6.14	6.84	7.64	7.64	1.84	2.50	3.46	4.34	4.39	5.30	6.10	6.70	7.33
X-n480-k70	1.71	2.45	3.23	3.91	4.47	5.06	5.56	6.05	6.49	1.66	2.44	3.28	3.88	4.45	5.10	5.61	6.17	6.37
X-n491-k59	1.73	2.46	3.16	3.68	4.32	4.61	5.04	5.38	5.55	1.74	2.51	3.19	3.84	4.54	4.93	5.30	5.71	6.18
Mean	1.70	2.44	3.07	3.68	4.21	4.67	5.15	5.54	5.82	1.73	2.44	3.13	3.76	4.25	4.73	5.19	5.58	5.95

Table A.12: Average speedup on large-sized $\mathbb X$ instances.

1.63 2.24 1.57 2.29 1.72 2.51 1.76 2.53 1.76 2.53 1.76 2.54 1.76 2.54 1.77 2.44 1.77 2.44 1.70 2.44 1.67 2.51 1.76 2.51 1.76 2.51 1.76 2.51 1.77 2.51 1.76 2.51 1.77 2.51	20		ı	(4	ı		(
1.63 2.24 1.57 2.29 3 1.72 2.51 1.76 2.53 1.76 2.50 1.69 2.50 1.63 2.35 9 1.76 2.54 1.75 2.51 1.70 2.44 1.67 2.51 1.70 2.44 1.67 2.51 1.76 2.51 1.76 2.51 1.77 2.51 1.78 2.51 1.79 2.51 1.76 2.51 1.76 2.51 1.77 2.		9	2	x	D.	10	2	3	4	ಬ	9	7	∞	6	10
1.57 2.29 1.72 2.51 1.76 2.53 1.76 2.52 1.69 2.50 1.63 2.35 1.76 2.54 1.75 2.51 1.76 2.51 1.76 2.51 1.76 2.51 1.76 2.51 1.76 2.51 1.76 2.51 1.76 2.51 1.77 2.51	3.37	3.69	4.02	4.41	4.65	4.93	1.59	2.26	2.78	3.23	3.67	4.02	4.38	4.66	4.84
1.72 2.51 1.76 2.53 1.76 2.53 1.69 2.50 1.63 2.35 1.76 2.54 1.75 2.51 1.77 2.44 1.67 2.51 1.76 2.51 1.76 2.51 1.76 2.51 1.76 2.51 1.77 2.51	3.23	3.64	4.03	4.49	4.62	4.95	1.61	2.26	2.69	3.32	3.67	3.89	4.35	4.77	4.95
1.76 2.53 1.76 2.52 1.69 2.50 1.63 2.35 1.76 2.54 1.75 2.51 1.70 2.44 1.67 2.51 1.76 2.51 1.76 2.51 1.76 2.51 1.76 2.51 1.76 2.51 1.77 2.51 1.78 2.51 1.79 2.51	3.76	4.26	4.82	5.23	5.55	6.03	1.75	2.48	3.14	3.86	4.30	4.87	5.31	5.70	6.11
1.76 2.52 1.69 2.50 1.63 2.35 1.76 2.54 1.75 2.51 1.70 2.44 1.67 2.51 1.76 2.51 1.76 2.51 1.76 2.51 1.76 2.51 1.76 2.51 1.77 2.51	3.92	4.26	4.80	5.37	5.86	6.03	1.79	2.56	3.28	3.95	4.73	5.31	5.71	6.47	6.80
1.69 2.50 1.63 2.35 1.76 2.54 1.75 2.51 1.70 2.44 1.67 2.51 1.76 2.51 1.76 2.51 1.76 2.51 1.76 2.51 1.77 2.51 1.78 2.51 1.79 2.40	3.91	4.55	5.10	5.68	6.02	6.36	1.72	2.46	3.20	3.73	4.37	4.86	5.22	5.73	6.03
1.63 2.35 1.76 2.54 1.84 2.59 1.75 2.51 1.70 2.44 1.67 2.51 1.76 2.51 1.69 2.40 1.78 2.55 1.79 2.51	3.68	4.28	4.64	5.07	5.40	5.58	1.67	2.43	3.01	3.71	4.13	4.55	5.02	5.14	5.53
1.76 2.54 1.84 2.59 1.75 2.51 1.70 2.44 1.67 2.51 1.76 2.51 1.76 2.51 1.69 2.40 1.76 2.55 1.73 2.37	3.47	3.81	4.47	5.01	5.09	5.36	1.67	2.35	2.92	3.48	3.71	4.34	4.71	4.94	4.85
1.84 2.59 1.75 2.51 1.70 2.44 1.67 2.51 1.76 2.51 1.76 2.51 1.69 2.40 1.76 2.55 1.73 2.37	4.22	4.75	5.18	5.52	6.17	6.79	1.74	2.75	3.46	4.40	5.05	5.80	6.32	88.9	7.40
1.75 2.51 1.70 2.44 1.67 2.51 1.76 2.51 1.76 2.51 1.69 2.40 1.76 2.55 1.73 2.37	4.17	4.88	5.36	5.89	6.54	09.9	1.76	2.60	3.23	4.07	4.61	5.06	5.78	6.01	6.50
1.70 2.44 1.67 2.51 1.76 2.51 1.76 2.51 1.69 2.40 1.76 2.55 1.73 2.37	3.78	4.37	4.79	5.29	5.56	5.84	1.71	2.42	3.15	3.84	4.34	4.88	5.25	5.57	5.92
1.67 2.51 1.76 2.51 1.76 2.51 1.69 2.40 1.76 2.55 1.73 2.37	3.71	4.26	4.61	5.15	5.58	5.63	1.71	2.34	3.04	3.57	4.05	4.66	5.07	5.40	5.61
1.76 2.51 1.76 2.51 1.69 2.40 1.76 2.55 1.73 2.37	3.80	4.31	4.64	5.33	5.71	6.15	1.69	2.50	3.16	3.61	4.27	4.80	5.06	5.86	5.86
1.76 2.51 1.69 2.40 1.76 2.55 1.73 2.37	3.87	4.54	5.17	5.58	00.9	6.50	1.75	2.46	3.18	3.88	4.44	5.05	5.56	6.11	6.34
1.69 2.40 1.76 2.55 1.73 2.37	3.77	4.37	4.93	5.39	5.89	6.20	1.70	2.38	3.17	3.84	4.42	5.11	5.35	6.05	6.13
1.76 2.55 1.73 2.37	3.49	4.19	4.54	4.91	5.24	5.56	1.66	2.41	3.03	3.71	4.27	4.78	5.07	5.53	5.77
1.73 2.37	3.79	4.44	4.99	5.45	5.93	6.18	1.72	2.42	3.11	3.65	4.29	4.85	5.17	5.69	5.93
1	3.69	4.10	4.54	4.89	5.26	5.54	1.62	2.29	2.86	3.40	3.82	4.29	4.60	4.84	5.16
2.53	3.92	4.58	5.02	5.68	80.9	6.54	1.77	2.60	3.17	4.15	4.77	5.23	5.93	6.39	6.71
	3.83	4.31	4.92	5.30	5.67	5.79	1.79	2.67	3.35	4.00	4.65	5.18	5.47	6.15	6.40
2.39	3.61	4.14	4.69	5.00	5.41	5.71	1.69	2.42	3.10	3.63	4.28	4.77	5.11	5.50	5.64
X-n783-k48 1.72 2.46 3.25	3.91	4.36	5.03	5.30	5.94	6.21	1.76	2.52	3.16	3.83	4.42	5.00	5.48	5.78	6.09
1.65 2.42	3.64	4.10	4.71	5.08	5.52	5.88	1.71	2.43	3.07	3.70	4.21	4.66	5.02	5.45	5.78
1.80 2.54	4.09	4.61	5.45	5.96	6.15	6.89	1.77	2.45	3.26	4.15	4.65	5.33	5.98	6.46	6.53
X-n837-k142 1.78 2.63 3.50	4.24	4.94	5.69	6.18	6.83	7.17	1.77	2.57	3.53	4.26	4.87	5.38	6.35	6.52	6.83
1.73 2.46	3.79	4.38	4.96	5.40	6.02	6.12	1.71	2.47	3.10	3.74	4.27	4.85	5.22	5.72	6.01
2.44	3.76	4.25	4.79	5.20	5.59	5.93	1.70	2.38	3.03	3.65	4.20	4.64	5.04	5.39	5.65
X-n895-k37 1.66 2.36 3.00	3.64	4.11	4.59	4.93	5.49	5.78	1.66	2.37	2.98	3.60	4.05	4.59	4.94	5.26	5.60
X-n916-k207 1.81 2.69 3.50	4.09	5.17	5.84	6.35	6.77	7.17	1.87	2.79	3.55	4.48	5.19	5.96	6.39	7.16	7.76
X-n936-k151 1.78 2.51 3.19	3.91	4.49	4.94	5.39	5.92	5.99	1.80	2.64	3.31	4.06	4.67	5.33	5.76	6.27	6.55
1.73 2.51	3.86	4.43	4.99	5.47	6.02	6.46	1.69	2.44	3.10	3.71	4.31	4.81	5.23	5.72	5.98
1 2.45	3.71	4.37	4.67	5.14	2.67	5.90	1.77	2.53	3.27	3.86	4.44	5.05	5.35	5.94	6.38
X-n1001-k43 1.75 2.45 3.13	3.85	4.27	5.01	5.39	5.78	6.17	1.72	2.42	3.01	3.77	4.24	4.76	5.15	5.62	5.84
Mean 1.72 2.47 3.13	3.78	4.33	4.84	5.29	5.71	6.02	1.72	2.46	3.13	3.78	4.32	4.85	5.27	5.71	5.98

Appendix A.2. Computational Details for the \mathbb{B} Instances

In the following, we report detailed results for the computations on the $\mathbb B$ dataset.

- Figure A.14 shows boxplots for the average gaps obtained by the approaches.
- Table A.13 shows the result of the one-tailed Wilcoxon signed rank test.
- Tables A.14 and A.15 report the computing time for the main algorithm procedures.
- Table A.16 shows the average gap for each instance in the dataset.
- Table A.17 shows the average speedup for each instance in the dataset.

Figure A.14: Average gaps obtained by FILO2 and FILO2 x (denoted by the number of solvers) on the $\mathbb B$ dataset when executing the standard (top) and long (bottom) versions. The median value is shown on the right of each boxplot.

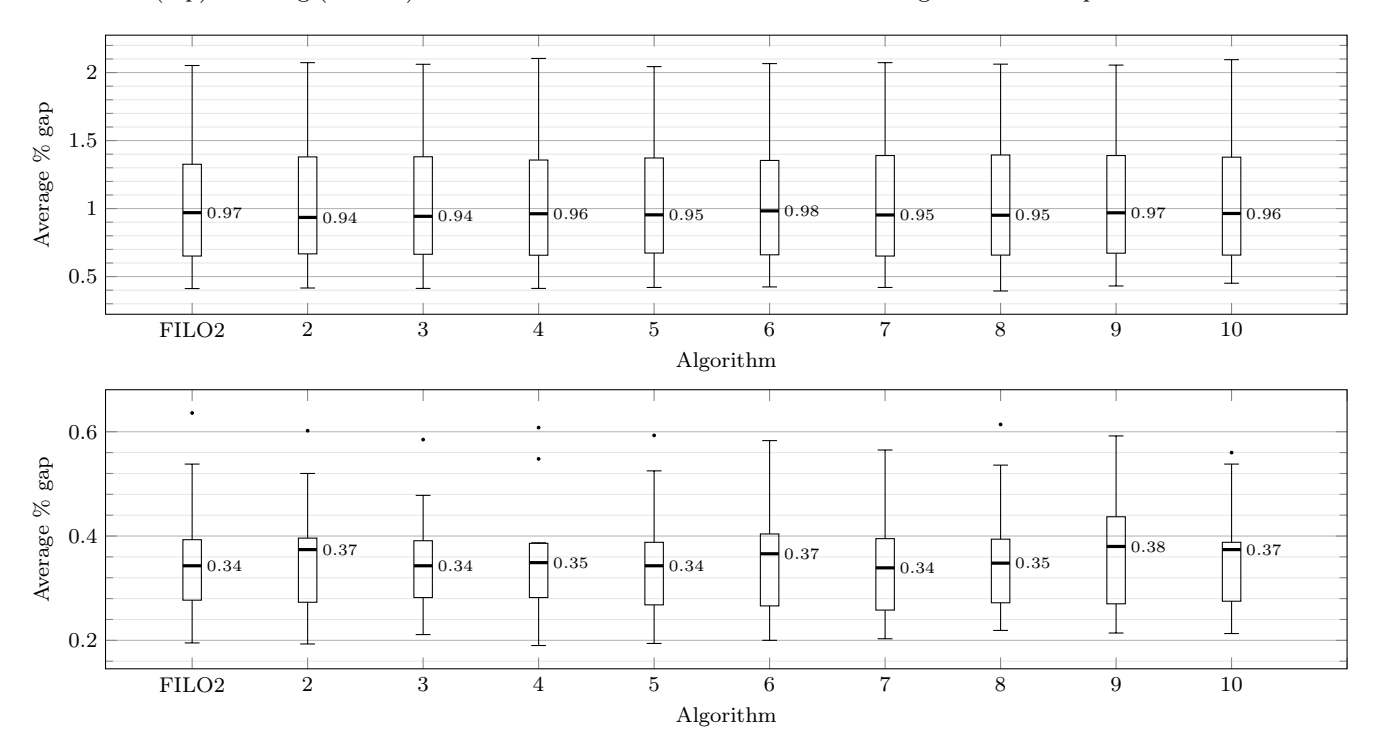


Table A.13: Computations on the $\mathbb B$ dataset: p-values for FILO2 x vs FILO2 on the left and FILO2 x (long) vs FILO2 (long) on the right.

p-values in bold are associated with rejected hypothesis when $\bar{\alpha}=0.002778.$

The last row of each group contains a p-value interpretation. In particular, FILO2 x is not statistically different from FILO2 when H_0 cannot be rejected (Similar), FILO2 x is statistically better when both H_0 and H_1 are rejected (Better), and, finally, FILO2 x is statistically worse when H_0 is rejected and H_1 is not rejected (Worse).

	$\mathrm{FILO2}^x$ vs FII	LO2		$FILO2^x$ (long) vs FII	LO2 (long)
Solvers	$H_0 \ / \ H_1$	Outcome		$H_0\ /\ H_1$	Outcome
2	$0.375000\ /\ 0.838867$	Similar	(0.695312 / 0.687500	Similar
3	$0.556641 \ / \ 0.753906$	Similar	($0.695312 \ / \ 0.687500$	Similar
4	$0.492188 \ / \ 0.784180$	Similar	($0.556641 \ / \ 0.753906$	Similar
5	$0.845703 \ / \ 0.615234$	Similar	($0.625000 \ / \ 0.312500$	Similar
6	$0.232422 \ / \ 0.903320$	Similar	($0.921875 \ / \ 0.577148$	Similar
7	$0.695312 \ / \ 0.687500$	Similar	(0.322266 / 0.161133	Similar
8	$0.695312 \ / \ 0.687500$	Similar		$1.000000 \ / \ 0.539062$	Similar
9	$0.083984 \ / \ 0.967773$	Similar	($0.625000 \ / \ 0.312500$	Similar
10	0.375000 / 0.838867	Similar	(0.769531 / 0.652344	Similar

Table A.14: Computing time in seconds for the main algorithm FILO2 and FILO2 x procedures when solving the $\mathbb B$ dataset.

					FIL	$O2^x$				
	FILO2	2	3	4	5	6	7	8	9	10
Instance preprocessing	2.55	1.37	0.92	0.70	0.57	0.49	0.42	0.37	0.33	0.31
Construction phase	0.10	0.10	0.10	0.10	0.10	0.10	0.10	0.10	0.10	0.10
Greedy route estimation	0.00	0.00	0.00	0.00	0.00	0.00	0.00	0.00	0.00	0.00
Move generators initialization	0.03	0.05	0.05	0.05	0.05	0.05	0.06	0.06	0.06	0.06
Route minimization procedure	0.60	0.54	0.54	0.55	0.55	0.55	0.55	0.55	0.56	0.57
Core optimization procedure	86.24	52.35	35.41	28.02	23.32	20.27	17.86	16.11	14.87	14.16

Table A.15: Computing time in seconds for the main algorithm FILO2 (long) and FILO2 x (long) procedures when solving the $\mathbb B$ dataset.

					FIL	$O2^x$				
	FILO2	2	3	4	5	6	7	8	9	10
Instance preprocessing	2.55	1.35	0.92	0.70	0.57	0.49	0.42	0.37	0.34	0.31
Construction phase	0.10	0.10	0.10	0.10	0.10	0.10	0.10	0.10	0.10	0.10
Greedy route estimation	0.00	0.00	0.00	0.00	0.00	0.00	0.00	0.00	0.00	0.00
Move generators initialization	0.03	0.05	0.05	0.05	0.05	0.06	0.06	0.06	0.06	0.06
Route minimization procedure	0.60	0.53	0.55	0.55	0.55	0.56	0.56	0.56	0.56	0.57
Core optimization procedure	1003.96	596.74	418.68	331.28	276.20	240.92	212.14	192.24	177.54	168.38

Table A.16: Average gap on the $\mathbb B$ instances.

						I	$FILO2^x$					FILO2				$\mathrm{FILO}2^x$	$O2^x \; (\mathrm{long})$	ng)			
Instance	$_{ m BKS}$	FILO2	2	3	4	2	9	2	8	6	10	(long)	2	3	4	5	9	7	8	6	10
Leuven1	192848	0.41	0.42	0.41	0.41	0.42	0.42	0.42	0.39	0.43	0.45	0.20	0.19	0.21	0.19	0.19	0.20	0.20	0.22	0.21	0.21
Leuven2	111391	0.93	0.85	0.87	0.91	0.91	0.97	0.92	0.89	0.95	0.92	0.30	0.37	0.32	0.32	0.32	0.34	0.30	0.33	0.45	0.38
Antwerp1	477277	0.52	0.52	0.54	0.52	0.51	0.53	0.51	0.53	0.53	0.51	0.22	0.24	0.24	0.25	0.24	0.23	0.22	0.24	0.25	0.23
Antwerp2	291350	1.01	1.08	1.03	1.06	1.06	1.09	1.05	1.08	1.08	1.07	0.39	0.40	0.39	0.38	0.37	0.39	0.39	0.37	0.37	0.39
Ghent1	469531	0.63	0.65	0.65	0.64	99.0	0.64	0.64	0.64	0.65	0.64	0.27	0.26	0.27	0.27	0.25	0.25	0.24	0.26	0.26	0.26
Ghent2	257748	1.42	1.48	1.50	1.46	1.48	1.44	1.50	1.50	1.49	1.48	0.40	0.38	0.37	0.37	0.39	0.41	0.40	0.40	0.39	0.37
Brussels1	501719	1.04	1.02	1.02	1.01	1.00	1.00	0.99	1.01	0.99	1.01	0.38	0.39	0.39	0.39	0.38	0.40	0.37	0.38	0.39	0.39
Brussels2	345468	1.89	1.86	1.87	1.93	1.90	1.89	1.93	1.89	1.91	1.91	0.54	0.52	0.48	0.55	0.52	0.55	0.55	0.54	0.51	0.54
Flanders1	7240118	0.72	0.72	0.71	0.72	0.73	0.72	0.70	0.71	0.73	0.71	0.31	0.31	0.32	0.31	0.31	0.30	0.30	0.31	0.30	0.32
Flanders2	4373244	2.05	2.07	2.06	2.10	2.04	2.07	2.07	2.06	2.06	2.09	0.64	09.0	0.59	0.61	0.59	0.58	0.57	0.61	0.59	0.56
Mean		1.06	1.07	1.07	1.08	1.07	1.08	1.07	1.07	1.08	1.08	0:36	0.37	0.36	0.37	0.36	0.36	0.36	0.36	0.37	0.36

Table A.17: Average speedup on the $\mathbb B$ instances.

				-	${ m FILO}2^x$								FIL	FILO2 x (lo	(long)			
Instance	2	3	4	25	9	7	∞	6	10	2	3	4	ಬ	9	2	∞	6	10
Leuven1	1.70	2.51	3.26	3.93	4.47	5.14	5.76	6.15	6.43	1.73	2.48	3.20	3.85	4.45	5.03	5.53	6.01	6.35
Leuven2	1.59		2.97	3.60	4.09	4.50	4.93	5.46	5.77	1.56	2.26	2.78	3.34	3.74	4.22	4.51	4.97	5.18
Antwerp1	1.71		3.31	3.98	4.68	5.30	6.02	6.57	6.62	1.74	2.52	3.24	3.94	4.53	5.17	5.73	6.22	6.58
Antwerp2	1.65		3.10	3.72	4.27	4.82	5.31	5.74	6.04	1.71	2.43	3.09	3.70	4.21	4.78	5.25	5.67	00.9
Ghent1	1.69		3.22	3.97	4.60	5.23	5.94	6.39	98.9	1.74	2.51	3.21	3.89	4.47	5.11	5.68	6.14	6.56
Ghent2	1.66		3.05	3.64	4.18	4.73	5.31	5.64	6.02	1.69	2.37	2.98	3.55	4.03	4.56	5.04	5.47	5.75
Brussels1	1.69		3.22	3.91	4.47	5.14	5.87	6.32	6.74	1.73	2.49	3.18	3.84	4.42	5.08	5.65	6.12	6.53
Brussels2	1.63		3.00	3.55	4.06	4.66	5.15	5.53	5.71	1.68	2.36	2.97	3.54	4.08	4.63	5.16	5.53	5.77
Flanders1	1.68		3.17	3.84	4.46	5.11	5.65	6.32	6.59	1.73	2.47	3.17	3.82	4.41	5.05	5.59	60.9	6.43
Flanders2	1.55	2.22	2.73	3.18	3.65	4.07	4.43	4.75	4.85	1.61	2.25	2.80	3.33	3.84	4.34	4.82	5.15	5.42
Mean	1.65	.65 2.44 3.08	3.08	3.69	4.24	4.81	5.35	5.79	6.05	1.68	2.40	3.03	3.63	4.17	4.73	5.22	5.65	5.96

Appendix A.3. Computational Details for the \mathbb{I} Instances

In the following, we report detailed results for the computations on the I dataset.

- Figure A.15 shows boxplots for the average gaps obtained by the approaches.
- Table A.18 shows the result of the one-tailed Wilcoxon signed rank test.
- Tables A.19 and A.20 report the computing time for the main algorithm procedures.
- Table A.21 shows the average gap for each instance in the dataset.
- Table A.22 shows the average speedup for each instance in the dataset.

Figure A.15: Average gaps obtained by FILO2 and FILO2 x (denoted by the number of solvers) on the $\mathbb I$ dataset when executing the standard (top) and long (bottom) versions. The median value is shown on the right of each boxplot.

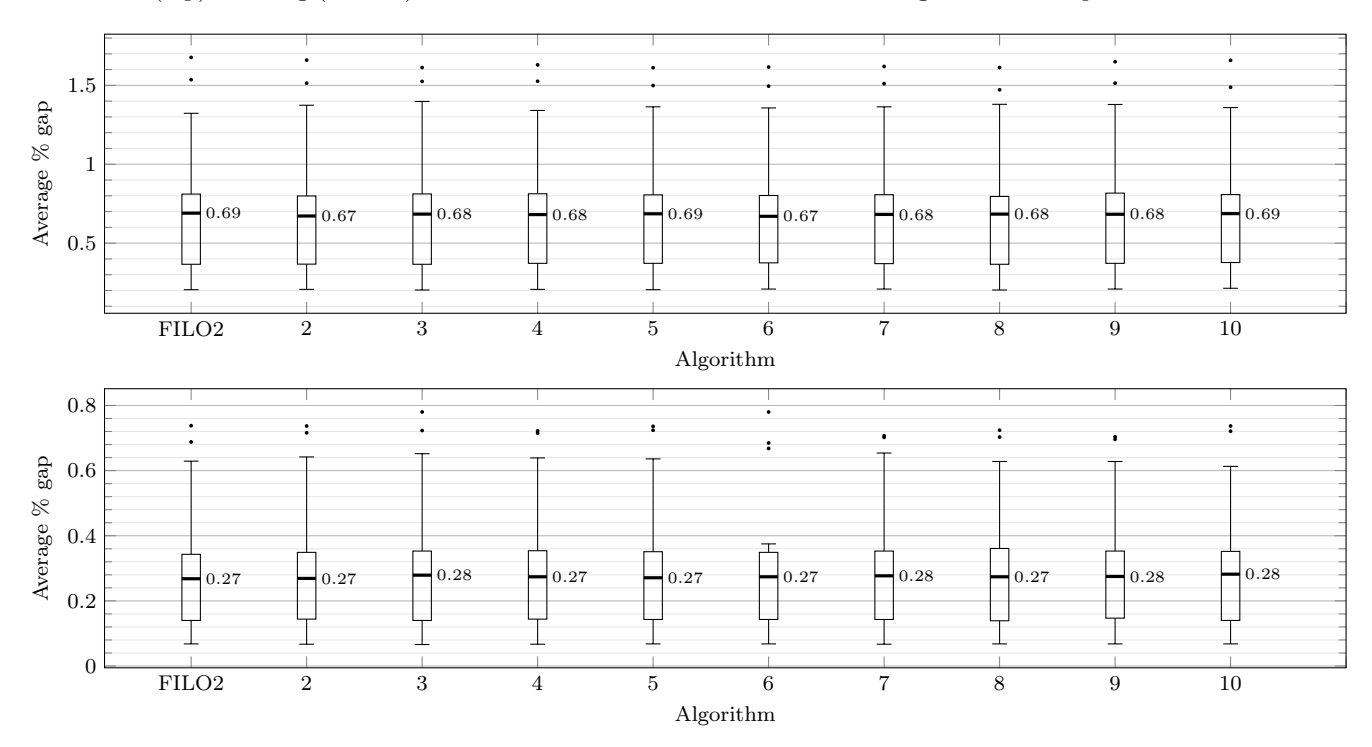


Table A.18: Computations on the \mathbb{I} dataset: p-values for FILO2 x vs FILO2 on the left and FILO2 x (long) vs FILO2 (long) on the right.

p-values in bold are associated with rejected hypothesis when $\bar{\alpha}=0.002778.$

The last row of each group contains a p-value interpretation. In particular, FILO2 x is not statistically different from FILO2 when H_0 cannot be rejected (Similar), FILO2 x is statistically better when both H_0 and H_1 are rejected (Better), and, finally, FILO2 x is statistically worse when H_0 is rejected and H_1 is not rejected (Worse).

	$\mathrm{FILO}2^x$ vs FII	LO2	$\mathrm{FILO2}^x$ (long) vs $\mathrm{FILO2}$ (long)
Solvers	$H_0 \ / \ H_1$	Outcome	H_0 / H_1 Outcome
2	$0.674223 \ / \ 0.337111$	Similar	$0.277355 \ / \ 0.869451$ Similar
3	$0.985435 \ / \ 0.492718$	Similar	0.082550 / 0.962074 Similar
4	$0.570597\ /\ 0.727062$	Similar	0.164957 / 0.923177 Similar
5	$0.956329 \; / \; 0.478165$	Similar	0.701181 / 0.662889 Similar
6	$0.898317 \ / \ 0.565256$	Similar	0.142906 / 0.933637 Similar
7	$0.985435 \ / \ 0.492718$	Similar	0.311794 / 0.852874 Similar
8	$0.927279 \ / \ 0.463639$	Similar	0.348810 / 0.835009 Similar
9	$0.570597\ /\ 0.727062$	Similar	0.294252 / 0.861322 Similar
10	$0.498009 \ / \ 0.762547$	Similar	0.521673 / 0.750996 Similar

Table A.19: Computing time in seconds for the main algorithm FILO2 and FILO2 x procedures when solving the $\mathbb I$ dataset.

					FIL	$\Im 2^x$				
	FILO2	2	3	4	5	6	7	8	9	10
Instance preprocessing	126.49	67.00	43.86	33.43	26.91	22.93	19.46	17.37	15.29	14.03
Construction phase	5.23	5.44	5.77	5.13	5.21	5.94	5.68	5.99	5.66	5.72
Greedy route estimation	3.37	3.35	3.34	3.34	3.34	3.35	3.34	3.35	3.34	3.35
Move generators initialization	3.60	4.09	4.03	4.08	4.24	4.88	4.83	5.33	5.14	5.31
Route minimization procedure	5.48	6.31	6.30	6.37	6.52	6.77	6.76	7.01	6.96	7.20
Core optimization procedure	166.58	100.68	69.74	55.33	46.99	41.36	36.50	34.10	31.18	29.86

Table A.20: Computing time in seconds for the main algorithm FILO2 (long) and FILO2 x (long) procedures when solving the $\mathbb I$ dataset.

					FILO	$O2^x$				
	FILO2	2	3	4	5	6	7	8	9	10
Instance preprocessing	126.53	65.51	44.04	33.46	26.93	22.87	19.46	17.39	15.29	14.08
Construction phase	5.23	5.18	5.65	5.16	5.22	5.84	5.63	5.96	5.68	5.76
Greedy route estimation	3.37	3.34	3.34	3.34	3.34	3.35	3.34	3.36	3.34	3.35
Move generators initialization	3.58	3.87	4.01	4.09	4.25	4.81	4.82	5.24	5.19	5.36
Route minimization procedure	5.48	6.11	6.28	6.39	6.51	6.70	6.75	7.02	6.98	7.24
Core optimization procedure	2349.73	1349.64	943.40	737.08	614.16	527.56	462.72	426.20	384.02	364.27

Table A.21: Average gap on the \mathbb{I} instances.

							$FILO2^x$					FILO2				FIL	$FILO2^x (long)$	ng)			
Instance	BKS	FILO2	2	3	4	22	9	7	∞	6	10	(long)	2	33	4	ಸಾ	9	7	∞	6	10
Valle-D-Aosta	21679514	0.27	0.26	0.26	0.26	0.24	0.25	0.25	0.27	0.26	0.25	0.13	0.14	0.14	0.13	0.14	0.14	0.13	0.13	0.13	0.13
Molise	111184982	0.41	0.41	0.42	0.42	0.41	0.42	0.42	0.41	0.42	0.42	0.16	0.15	0.14	0.15	0.15	0.16	0.16	0.15	0.15	0.15
Trentino-Alto-Adige	102063181	0.89	0.89	0.91	0.92	0.90	0.89	0.90	0.90	0.92	0.91	0.36	0.36	0.38	0.37	0.37	0.35	0.37	0.39	0.36	0.37
Basilicata	175623919	0.74	0.69	0.73	0.70	0.71	0.68	0.70	0.71	0.70	0.73	0.31	0.30	0.30	0.29	0.30	0.29	0.30	0.30	0.33	0.29
Umbria	545507981	0.28	0.28	0.28	0.29	0.29	0.28	0.29	0.28	0.28	0.29	0.13	0.13	0.13	0.13	0.13	0.13	0.13	0.13	0.12	0.13
Abruzzo	311712556	0.70	0.73	0.74	0.73	0.74	0.74	0.72	0.74	0.74	0.72	0.26	0.26	0.27	0.27	0.26	0.27	0.27	0.26	0.27	0.27
Friuli-Venezia-Giulia	415805616	0.62	0.63	0.65	0.64	0.65	0.64	0.64	0.64	0.66	0.64	0.28	0.28	0.29	0.28	0.29	0.28	0.28	0.28	0.28	0.29
Liguria	1426389867	0.21	0.21	0.20	0.21	0.21	0.21	0.21	0.20	0.21	0.21	0.07	0.07	0.02	0.07	0.02	0.07	0.07	0.07	0.07	0.07
Calabria	1964651530	0.38	0.38	0.38	0.39	0.39	0.39	0.38	0.38	0.39	0.39	0.13	0.14	0.14	0.13	0.13	0.14	0.13	0.13	0.14	0.14
Marche	420484426	0.68	0.65	0.67	0.66	0.67	0.66	0.66	0.67	0.67	29.0	0.25	0.25	0.24	0.24	0.24	0.24	0.24	0.24	0.24	0.24
Sardegna	827934149	1.68	1.66	1.61	1.63	1.61	1.62	1.62	1.61	1.65	1.66	0.74	0.74	0.78	0.72	0.72	0.78	0.70	0.72	0.70	0.74
Campania	391859276	1.04	1.02	1.01	1.01	1.02	1.01	1.03	1.02	1.01	1.01	0.40	0.37	0.38	0.38	0.37	0.38	0.38	0.39	0.38	0.38
Piemonte	2627446164	0.32	0.33	0.33	0.33	0.32	0.33	0.33	0.33	0.33	0.33	0.15	0.15	0.15	0.15	0.15	0.15	0.15	0.15	0.15	0.15
$\operatorname{Toscana}$	1084417188	0.78	0.77	0.78	0.78	0.77	0.77	0.78	0.76	0.78	0.77	0.33	0.32	0.33	0.33	0.33	0.35	0.33	0.34	0.35	0.33
Puglia	1464797603	1.54	1.51	1.53	1.53	1.50	1.49	1.51	1.47	1.51	1.49	0.69	0.72	0.72	0.72	0.74	0.68	0.71	0.70	0.70	0.72
Sicilia	1774262462	1.32	1.37	1.40	1.34	1.36	1.36	1.36	1.38	1.38	1.36	0.63	0.64	0.65	0.64	0.64	0.67	0.65	0.63	0.63	0.61
Veneto	1050488613	0.72	0.70	0.70	0.71	0.70	0.72	0.71	0.70	0.70	0.71	0.30	0.29	0.30	0.29	0.29	0.29	0.29	0.29	0.28	0.29
Emilia-Romagna	5405446715	0.24	0.24	0.24	0.24	0.24	0.24	0.23	0.24	0.24	0.24	0.09	0.09	0.09	0.09	0.09	0.09	0.09	0.09	0.09	0.09
Lombardia	1339900081	0.75	0.77	0.76	0.75	0.75	0.76	0.77	0.76	0.75	0.76	0.34	0.35	0.35	0.35	0.34	0.34	0.35	0.35	0.35	0.35
Lazio	3145381332	0.40	0.39	0.40	0.40	0.40	0.40	0.40	0.40	0.40	0.40	0.14	0.14	0.15	0.15	0.15	0.14	0.15	0.14	0.15	0.14
Mean		0.70	0.70	0.70	0.70	69.0	69.0	0.70	69.0	0.70	0.70	0.29	0.30	0.30	0.29	0.29	0.30	0.29	0:30	0.29	0.29

Table A.22: Average speedup on the $\mathbb I$ instances.

					$FILO2^x$								FIL	$FILO2^x (long)$	ng)			
Instance	2	3	4	5	9	2	∞	6	10	2	3	4	5	9	2	∞	6	10
Valle-D-Aosta	1.69	2.37	3.00	3.59	4.09	4.65	5.00	5.57	5.84	1.69	2.42	3.07	3.70	4.23	4.85	5.29	5.82	6.16
Molise	1.66	2.43	3.06	3.62	4.15	4.64	5.01	5.53	5.77	1.75	2.53	3.25	3.95	4.58	5.22	5.75	6.35	6.73
Trentino-Alto-Adige	1.54	2.19	2.68	3.12	3.49	3.93	4.13	4.48	4.62	1.68	2.36	2.98	3.55	4.12	4.68	5.07	5.57	5.85
Basilicata	1.67	2.29	2.82	3.29	3.65	4.10	4.31	4.65	4.76	1.72	2.46	3.13	3.76	4.38	4.96	5.37	5.96	6.25
Umbria	1.70	2.43	3.05	3.60	4.04	4.56	4.90	5.36	5.57	1.75	2.52	3.24	3.92	4.55	5.21	5.67	6.27	6.63
Abruzzo	1.65	2.25	2.78	3.20	3.54	3.99	4.18	4.51	4.70	1.69	2.36	2.99	3.53	4.13	4.59	4.96	5.48	5.71
Friuli-Venezia-Giulia	1.61	2.29	2.85	3.28	3.67	4.07	4.31	4.62	4.84	1.71	2.38	3.01	3.56	4.20	4.71	5.07	5.54	5.91
Liguria	1.72	2.44	3.04	3.60	3.98	4.53	4.81	5.20	5.34	1.77	2.53	3.28	3.96	4.57	5.24	5.71	6.34	6.67
Calabria	1.67	2.38	2.95	3.44	3.80	4.22	4.47	4.86	4.99	1.76	2.53	3.25	3.91	4.53	5.13	5.64	6.23	6.57
Marche	1.62	2.30	2.88	3.34	3.70	4.11	4.29	4.75	4.80	1.70	2.41	3.03	3.61	4.19	4.74	5.09	5.56	5.85
Sardegna	1.64	2.32	2.87	3.30	3.64	4.01	4.14	4.56	4.68	1.75	2.51	3.18	3.83	4.42	5.01	5.45	5.98	6.31
Campania	1.62	2.33	2.87	3.34	3.68	4.11	4.35	4.65	4.87	1.72	2.46	3.10	3.68	4.22	4.83	5.17	5.82	6.05
Piemonte	1.67	2.36	2.92	3.37	3.65	4.10	4.31	4.62	4.77	1.76	2.53	3.25	3.89	4.53	5.11	5.57	6.13	6.48
Toscana	1.69	2.37	2.94	3.37	3.68	4.11	4.31	4.68	4.81	1.76	2.55	3.24	3.94	4.49	5.13	5.51	6.13	6.51
Puglia	1.67	2.34	2.88	3.32	3.59	4.00	4.12	4.45	4.59	1.76	2.51	3.22	3.84	4.42	5.00	5.39	5.97	6.26
Sicilia	1.65	2.33	2.88	3.31	3.66	3.98	4.12	4.47	4.61	1.75	2.49	3.17	3.74	4.35	4.97	5.29	5.81	6.11
Veneto	1.71	2.40	2.96	3.42	3.71	4.13	4.29	4.69	4.85	1.76	2.46	3.16	3.71	4.29	4.86	5.28	5.78	6.02
Emilia-Romagna	1.68	2.32	2.82	3.23	3.44	3.82	4.01	4.25	4.42	1.76	2.52	3.22	3.87	4.41	5.04	5.42	6.05	6.34
Lombardia	1.68	2.37	2.92	3.37	3.61	4.07	4.24	4.60	4.72	1.76	2.50	3.21	3.84	4.42	5.10	5.48	6.20	6.45
Lazio	1.67	2.30	2.80	3.21	3.43	3.76	3.90	4.21	4.31	1.77	2.54	3.23	3.87	4.47	5.04	5.45	6.01	6.34
Mean	1.66	2.34	2.89	3.35	3.66	4.08	4.27	4.62	4.78	1.74	2.48	3.16	3.78	4.37	4.96	5.37	5.94	6.24

References

- M. F. Abdelatti and M. S. Sodhi. An improved gpu-accelerated heuristic technique applied to the capacitated vehicle routing problem. In *GECCO '20: Proceedings of the 2020 Genetic and Evolutionary Computation Conference*, pages 663—671. ACM, 2020.
- L. Accorsi and D. Vigo. Routing one million customers in a handful of minutes. *Computers & Operations Research*, 164:106562, 2024.
- Luca Accorsi and Daniele Vigo. A fast and scalable heuristic for the solution of large-scale capacitated vehicle routing problems. *Transportation Science*, 55(4):832–856, 2021. doi: 10.1287/trsc.2021.1059. URL https://doi.org/10.1287/trsc.2021.1059.
- Enrique Alba. Parallel Metaheuristics: A New Class of Algorithms. Wiley-Interscience, USA, 2005.
- F. Arnold, M. Gendreau, and K. Sörensen. Efficiently solving very large-scale routing problems. Computers & Operations Research, 107:32-42, 2019.
- P. Augerat, J. M. Belenguer, E. Benavent, Á. Corberán, D. Naddef, and G. Rinaldi. Computational results with a branch and cut code for the capacitated vehicle routing problem. *IMAG*, 34, 1995.
- D. Barbucha. Solving the capacitated vehicle routing problem by a team of parallel heterogeneous cooperating agents. In P. Jędrzejowicz, N. T. Nguyen, and K. Hoang, editors, *Computational Collective Intelligence. Technologies and Applications*, pages 332–341, Berlin, Heidelberg, 2011. Springer Berlin Heidelberg.
- D. Barbucha. A Cooperative Agent-Based Multiple Neighborhood Search for the Capacitated Vehicle Routing Problem, pages 129–143. Springer International Publishing, Cham, 2014.
- O. Beek, B. Raa, W. Dullaert, and D. Vigo. An efficient implementation of a static move descriptor-based local search heuristic. *Computers & Operations Research*, 94:1 10, 2018.
- Jon Louis Bentley. K-d trees for semidynamic point sets. In *Proceedings of the sixth annual symposium on Computational geometry*, pages 187–197, 1990.
- Z. Borčinová. Solving the capacitated vehicle routing problem using a parallel micro genetic algorithm. In 2018 IEEE Workshop on Complexity in Engineering (COMPENG), pages 1–6, 2018.
- Jan Christiaens and Greet Vanden Berghe. Slack induction by string removals for vehicle routing problems. *Transportation Science*, 54(2):417–433, 2020. doi: 10.1287/trsc.2019.0914. URL https://doi.org/10.1287/trsc.2019.0914.
- N. Christofides, , and S. Eilon. An algorithm for the vehicle-dispatching problem. *Journal of the Operational Research Society*, 20:309–318, 1969.
- N. Christofides, A. Mingozzi, P. Toth, and C. Sandi. Combinatorial Optimization. John Wiley, Chichester, 1979.
- N. Christofides, A. Mingozzi, and P. Toth. Exact algorithms for the vehicle routing problem, based on spanning tree and shortest path relaxations. *Mathematical Programming*, 20:255—-282, 1981.
- G. Clarke and J. W. Wright. Scheduling of vehicles from a central depot to a number of delivery points. *Operations Research*, 12(4):568—581, 1964.
- T. G. Crainic. Parallel Computation, Co-operation, Tabu Search, pages 283-302. Springer US, Boston, MA, 2005.
- T. G. Crainic. Parallel Solution Methods for Vehicle Routing Problems, pages 171–198. Springer US, Boston, MA, 2008.
- T. G. Crainic and N. Hail. *Parallel Metaheuristics Applications*, chapter 19, pages 447–494. John Wiley & Sons, Ltd, 2005
- T. G. Crainic and M. Toulouse. Explicit and emergent cooperation schemes for search algorithms. In V. Maniezzo, R. Battiti, and J.-P. Watson, editors, *Learning and Intelligent Optimization*, pages 95–109, Berlin, Heidelberg, 2008. Springer Berlin Heidelberg.
- T. G. Crainic and M. Toulouse. Parallel Meta-heuristics, pages 497–541. Springer US, Boston, MA, 2010.

- T. G. Crainic, M. Gendreau, and J.-Y. Potvin. *Parallel Tabu Search*, chapter 13, pages 289–313. John Wiley & Sons, Ltd, 2005.
- T. G. Crainic, Le C. Bertrand, and C. Roucairol. *Parallel Branch-and-Bound Algorithms*, chapter 1, pages 1–28. John Wiley & Sons, Ltd, USA, 2006.
- CVRPLIB. Capacitated vehicle routing problem library, 2025. URL http://vrp.galgos.inf.puc-rio.br/index.php/en/. visited on 2024-09-24.
- G. B. Dantzig and J. H. Ramser. The truck dispatching problem. Management Science, 6(1):80—91, 1959.
- K. F. Doerner, R. F. Hartl, G. Kiechle, M. Lucka, and M. Reimann. Parallel ant systems for the capacitated vehicle routing problem. In J. Gottlieb and G. R. Raidl, editors, *Evolutionary Computation in Combinatorial Optimization*, pages 72–83, Berlin, Heidelberg, 2004. Springer Berlin Heidelberg.
- O. J. Dunn. Multiple comparisons among means. Journal of the American Statistical Association, 56(293):52–64, 1961.
- M. L. Fisher. Optimal solution of vehicle routing problems using minimum k-trees. *Operations Research*, 42(4): 626–642, 1994.
- B. Gendron and T. G. Crainic. Parallel branch-and-branch algorithms: Survey and synthesis. *Operations Research*, 42(6):1042–1066, 1994.
- B. E. Gillett and J. G. Johnson. Multi-terminal vehicle-dispatch algorithm. Omega, 4(6):711–718, 1976.
- Fred Glover. Ejection chains, reference structures and alternating path methods for traveling salesman problems. *Discrete Applied Mathematics*, 65(1):223 253, 1996. ISSN 0166-218X. doi: 10.1016/0166-218X(94)00037-E. URL http://www.sciencedirect.com/science/article/pii/0166218X9400037-E. First International Colloquium on Graphs and Optimization.
- B. L. Golden, E. A. Wasil, J. P. Kelly, and I-M. Chao. The Impact of Metaheuristics on Solving the Vehicle Routing Problem: Algorithms, Problem Sets, and Computational Results, pages 33–56. Springer US, Boston, MA, 1998.
- P. Kalatzantonakis, A. Sifaleras, and N. Samaras. Cooperative versus non-cooperative parallel variable neighborhood search strategies: a case study on the capacitated vehicle routing problem. *Journal of Global Optimization*, 78 (2):327–348, 2005.
- G. A. P. Kindervater and J. K. Lenstra. An introduction to parallelism in combinatorial optimization. *Discrete Applied Mathematics*, 14(2):135–156, 1986.
- S. Kirkpatrick, C. D. Gelatt, and M. P. Vecchi. Optimization by simulated annealing. *Science*, 220(4598):671-680, 1983. ISSN 0036-8075. doi: 10.1126/science.220.4598.671. URL https://science.sciencemag.org/content/220/4598/671.
- J. Kytöjoki, T. Nuortio, O. Bräysy, and M. Gendreau. An efficient variable neighborhood search heuristic for very large scale vehicle routing problems. *Computers & Operations Research*, 34(9):2743–2757, 2007.
- G. Laporte, M. Gendreau, J.-Y. Potvin, and F. Semet. Classical and modern heuristics for the vehicle routing problem. *International Transactions in Operational Research*, 7(4):285–300, 2000.
- F. Li, B. Golden, and E. Wasil. Very large-scale vehicle routing: new test problems, algorithms, and results. *Computers & Operations Research*, 32(5):1165–1179, 2005.
- H. R. Lourenço, O. C. Martin, and T. Stützle. Iterated Local Search, pages 320–353. Springer US, Boston, MA, 2003.
- Vinícius R. Máximo, Jean-François Cordeau, and Mariá C. V. Nascimento. Ails-ii: An adaptive iterated local search heuristic for the large-scale capacitated vehicle routing problem. *INFORMS Journal on Computing*, 36(4):974–986, 2024. doi: 10.1287/ijoc.2023.0106. URL https://doi.org/10.1287/ijoc.2023.0106.
- N. Mladenović and P. Hansen. Variable neighborhood search. Computers & Operations Research, 24(11):1097–1100, 1997. ISSN 0305-0548. doi: https://doi.org/10.1016/S0305-0548(97)00031-2. URL https://www.sciencedirect.com/science/article/pii/S0305054897000312.

- M. Rajesh Pandian, S. Somesh, and N. S. Rupesh, N. Narayanaswamy. Effective parallelization of the vehicle routing problem. In *GECCO '23: Proceedings of the Genetic and Evolutionary Computation Conference*, pages 1036—1044. ACM, 2023.
- Gerhard Reinelt and Giovanni Rinaldi. The traveling salesman problem. 1994.
- F. Semet, P. Toth, and D. Vigo. Chapter 2: Classical Exact Algorithms for the Capacitated Vehicle Routing Problem, pages 37–57. Society for Industrial and Applied Mathematics, 2014.
- Éric Taillard, Philippe Badeau, Michel Gendreau, François Guertin, and Jean-Yves Potvin. A tabu search heuristic for the vehicle routing problem with soft time windows. *Transportation Science*, 31(2):170–186, 1997. doi: 10.1287/trsc.31.2.170. URL https://doi.org/10.1287/trsc.31.2.170.
- El-Ghazali Talbi. Parallel Combinatorial Optimization (Wiley Series on Parallel and Distributed Computing). Wiley-Interscience, USA, 2006.
- Paolo Toth and Daniele Vigo, editors. *The Vehicle Routing Problem*. Society for Industrial and Applied Mathematics, 2002.
- Paolo Toth and Daniele Vigo. The granular tabu search and its application to the vehicle-routing problem. *INFORMS Journal on Computing*, 15(4):333-346, 2003. doi: 10.1287/ijoc.15.4.333.24890. URL https://doi.org/10.1287/ijoc.15.4.333.24890.
- E. Uchoa, D. Pecin, A. Pessoa, M. Poggi, T. Vidal, and A. Subramanian. New benchmark instances for the capacitated vehicle routing problem. *European Journal of Operational Research*, 257(3):845–858, 2017.
- Thibaut Vidal. Hybrid genetic search for the cvrp: Open-source implementation and swap* neighborhood. *Comput. Oper. Res.*, 140(C), 4 2022. ISSN 0305-0548. doi: 10.1016/j.cor.2021.105643. URL https://doi.org/10.1016/j.cor.2021.105643.
- F. Wilcoxon. Individual comparisons by ranking methods. Biometrics Bulletin, 1(6):80-83, 1945.
- P. Yelmewad and B. Talawar. Parallel version of local search heuristic algorithm to solve capacitated vehicle routing problem. *Cluster Computing*, 24(4):3671–3692, 2021.
- E. E. Zachariadis and C. T. Kiranoudis. A strategy for reducing the computational complexity of local search based methods for the vehicle routing problem. *Computers & Operations Research*, 37(12):2089–2105, 2010.